D3 - STATE OF THE ART REVIEW

SOUTH AFRICA DROUGHT MONITORING (ANIN)

Prepared by:	VITO
Approved by:	Beatriz Revilla-Romero
Authorized by:	Juan Suárez
Code:	D3
Version:	v2
Date:	02/03/2023
Internal code:	N/A

esa gmv vito AgroApps Hatfield

DOCUMENT STATUS SHEET

Version	Date	Pages	Changes
v1	13/01/2023	60	First version of the document
v2	02/03/2023	48	Revision according to the feedback received form ESA. All RIDs from MS1 implemented

TABLE OF CONTENTS

LIST OF TABLES AND FIGURES

1. INTRODUCTION

1.1. PURPOSE

D3 State-of-the-art review report highlights the relevant EO-based methods and solutions and provides a comprehensive review of the state-of-the-art of EO-based datasets and information technology with direct relevance to the drought monitoring has been performed. This document will be publicly available on the project website at http://drought-za.org/.

1.2. SCOPE

The document describes the concept and framework for drought monitoring and early warning systems in context to Africa and South Africa 3.1, available tools for drought monitoring 3.2 an overview of international and non-governmental early warning systems 3.3, GAP analysis 3.5 and conclusions 3.6. The scope of the document is to provide a comprehensive overview and baseline for the work to be performed in WP200

1.3. DEFINITIONS AND ACRONYMS

1.3.1. DEFINITIONS

Concepts and terms used in this document and needing a definition are included in the following table:

Table 1-1 Definitions

Concept / Term	Definition
dekad	ten days

1.3.2. ACRONYMS

Acronyms used in this document and needing a definition are included in the following table:

Table 1-2 Acronyms

Acronym	Definition
AEZ	Agroecological Zone
ARC	Agricultural Research Council
ARC-ISCW	Agricultural Research Council - Institute for Soil, Climate, and Water
ASTER	Advanced Spaceborne Thermal Emission and Reflection Radiometer
AVHRR	Advanced Very-High-Resolution Radiometer
CCSM	Community Climate System Model
CDR	Climate Data Record
CFSv2	Climate Forecast System Version 2
CHIRPS	Climate Hazards Group InfraRed Precipitation with Station
CICE	Community of Ice CodE
CNES	Centre National d'Études Spatiales
CONUS	Contiguous U.S.
CPT	Climate Predictability
CRID	Coarse Resolution Satellite Imagery Database
CRU	Climatic Research Unit
CS	coastal savanna
CWSI	crop water stress index
ECMWF	European Centre for Medium-Range Weather Forecasts
ECOSTRESS	Ecosystem Spaceborne Thermal Radiometer Experiment on Space Station

Acronym	Definition
EDA	Ensemble of Data Assimilations
ERA5	ECMWF reanalysis V5
EROS	Earth Resources Observation Satellite
ESA	European Space Agency
ESI	Evaporative Stress Index
ESMF	Earth System Modeling Framework
ET	evapotranspiration
EVI	Enhanced Vegetation Index
fAPAR	fraction of Absorbed Photosynthetically Active Radiation
Fcover	Fraction of Vegetation Cover
FEWS NET	Famine Early Warning Systems Network
FLOR	Forecast-oriented Low Ocean Resolution
GCOS	Global Climate Observing System
GEDI	Global Ecosystem Dynamics Investigation
GEOS	Goddard Earth Observing System
GFDL	Geophysical Fluid Dynamic
GMAO	Global Modeling and Assimilation Office
GMI	GPM Microwave Imager
GPCC	Global Precipitation Climatology Centre
GPM	Global Precipitation Measurement
GPS	Global Positioning System
GRACE	Gravity Recovery and Climate Experiment
GRACE-FO	Gravity Recovery and Climate Experiment Follow-On
HISUI	Hyperspectral Imager Suite
IFS	Integrated Forecast System
IR	Infrared
ISRO	Indian Space Research Organization
ISS	International Space Station
IVs	Inland Valleys
JAXA	Japan Aerospace Exploration Agency
KBDI	Keetch-Byram Drought Index
LAI	Leaf area index
LiDAR	Light Detection And Ranging
LP DAAC	Land Processes Distributed Active Archive Center
LST	land-surface temperature
MCDA	Multi Criteria Decision Analysis
McICA	Monte Carlo Independent Column Approximation
METRIC	Mapping EvapoTranspiration at high Resolution with Internalized Calibration
MODIS	Moderate Resolution Imaging Spectroradiometer
MSG	Meteosat Second Generation
MSZ	Moist Savanna Zone
NASA	National Aeronautics and Space Administration
NASS	National Agricultural Statistics Service Information
NCAR	National Center for Atmospheric Research
NCAS	National Centre for Atmospheric Science
NCEP	National Centers for Environmental Prediction
NDVI	Normalized Difference Vegetation Index

Acronym	Definition
NDWI	Normalized Difference Water Index
NEMO	Nucleus for European Modelling of the Ocean
NESDIS	National Environmental Satellite, Data, and Information Service
NGO	non-governmental organization
NIR	near-infrared
NIWIS	National Integrated Water Information System
NMME	North American Multi-Model Ensemble
NMSs	National Meteorological Services
NOAA	National Oceanic and Atmospheric Administration
OCO-3	Orbiting Carbon Observatory
OGCM	Ocean General Circulation Model
PASG	Percentage of Average Seasonal Greenness
PET	potential evapotranspiration
RPN	Recherche en Prévision Numérique
RRTM	Rapid Radiation Transfer Model
SAVI	Soil-Adjusted Vegetation Index
SEB	surface energy balance
SMA	Soil Moisture Anomaly
SMAP	Soil Moisture Active Passive
SMOS	Soil Moisture and Ocean Salinity
SPEI	Standardized Precipitation Evapotranspiration Index
SPI	Standardized Precipitation Index
SVI	Standardized Vegetation Index
SWIR	shortwave infrared reflectance
SYNOP	surface synoptic observations
TCI	Temperature Condition Index
TIR	Thermal infrared
TRMM	Tropical Rainfall Measuring Mission
TS	Time Series
UAS	Unmanned aircraft systems
UAV	Unmanned Aerial Vehicle
USAID	United States Agency for International Development
USDA	United States Department of Agriculture
USDM	U.S. Drought Monitor
VCI	Vegetation Condition Index
VHI	Vegetation Health Index
VNIR	visible near-infrared reflectance
VPD	vapor pressure deficit
WaPOR	Water Productivity Open-access portal

2. REFERENCES

2.1. APPLICABLE DOCUMENTS

The following documents, of the exact issue shown, form part of this document to the extent specified herein. Applicable documents are those referenced in the Contract or approved by the Approval Authority. They are referenced in this document in the form [AD.x]:

Table 2-1 Applicable Documents

Ref.	Title	Code	Version	Date
[AD.1]	Statement of Work. EO AFRICA - NATIONAL INCUBATORS EXPRO+	ESA-EOP-SD-SOW-0249	1.0	26/10/2021
[AD.2]	Proposal EO AFRICA NATIONAL INCUBATORS (ANIN)	GMV10277/22 V1/22,	1.0	18/02/2022

2.2. REFERENCE DOCUMENTS

The following documents, although not part of this document, amplify or clarify its contents. Reference documents are those not applicable and referenced within this document. They are referenced in this document in the form [RD.x]:

Table 2-2 Reference Documents

Ref.	Title	Code	Version	Date
[RD.1]	Food Security			2020-11-30
[RD.2]	Gary Bickel; Mark Nord; Cristofer Price; William Hamilton; John Cook (2000). "Guide to Measuring Household Food Security" (PDF). USDA Food and Nutrition Service.			
[RD.3]	United Nations, "Transforming our World: The 2030 Agenda for Sustainable Development," 2015.			
[RD.4]	Barrett, C. B. (11 February 2010). "Measuring Food Insecurity". Science. 327 (5967): 825–828. Bibcode:2010Sci...327..825B.			
[RD.5]	Gregory, P. J.; Ingram, J. S. I.; Brklacich, M. (29 November 2005). "Climate change and food security". Philosophical Transactions of the Royal Society B: Biological Sciences. 360 (1463): 2139–2148.			
[RD.6]	Varghese, D.; Radulović, M.; Stojković, S.; Crnojević, V. Reviewing the Potential of Sentinel-2 in Assessing the Drought. Remote Sens. 2021, 13, 3355. https:// doi.org/10.3390/rs13173355.			
[RD.7]	Masih et al., 2014. A review of droughts on the African continent: a geospatial and long-term perspective. Hydrol. Earth. Syst. Sci., 18, 3635-3649. doi:10.5194/hess-18-3635-2014.			
[RD.8]	Kim S-K., Shin, J, An, S-II, Kim H-J, Im, N., Xie, S-P., Kug, J-S., Yeh S-W. 2022. Widespread irreversible changes in surface temperature and precipitation in response to CO2 forcing. Nature Climate Change, 12: 834-840. /doi.org/10.1038/s41558-022-01452-z.			
[RD.9]	Conference on Water Scarcity in Africa: Issues and Challenges			2016-04-01
[RD.10]	https://gaez.fao.org/			2022-12-08
[RD.11]	https://worldclim.org/data/monthlywth.html			2022-12-08
[RD.12]	https://icesat.gsfc.nasa.gov/icesat/tools/SRTM30_Documentation.html			2022-12-08
[RD.13]	https://www.fao.org/3/ap658e/ap658e.pdf			
[RD.14]	Günther Fischer, Harrij Van Velthuizen, Eva Hizsnyik, and David Wiberg. 2009. Potentially Obtainable Yields in the Semi-Arid Tropics. Global Theme on Agroecosystems Report no. 54 Patancheru 502 324, Andhra Pradesh, India; International Crops Research Institute for the Semi-Arid Tropics. 68 pp.			
[RD.15]	https://interactive-atlas.ipcc.ch/			2022-12-08

Ref.	Title	Code	Version	Date
[RD.16]	Kim, SK., Shin, J., An, SI. et al. Widespread irreversible changes in surface temperature and precipitation in response to CO2 forcing. Nat. Clim. Chang. 12, 834–840 (2022)			
[RD.17]	https://gpm.nasa.gov/			2022-12-08
[RD.18]	https://disc.gsfc.nasa.gov/			2023-02-14
[RD.19]	https://public.wmo.int/en/media/press-release/early-warnings-all-action-plan-unveiled-cop27			2022-12-08
[RD.20]	https://www.undrr.org/terminology/early-warning-system			2022-11-24
[RD.21]	Masih et al., 2014. A review of droughts on the African continent: a geospatial and long-term perspective. Hydrol. Earth. Syst. Sci., 18, 3635-3649. doi:10.5194/hess-18-3635-2014.			
[RD.22]	https://climas.arizona.edu/blog/climate-models-versus-weather-models-different-approaches-different-needs			2022-11-28
[RD.23]	https://www.ecmwf.int/en/forecasts			2022-11-28
[RD.24]	https://www.ecmwf.int/en/forecasts/quality-our-forecasts/monitoring-observing-system			2022-11-28
[RD.25]	https://www.ncei.noaa.gov/access/metadata/landing-page/bin/iso?id=gov.noaa.ncdc:C00877#:~:text=The%20Climate%20Forecast%20System%20Version,Earth's%20oceans%2C%20land%20and%20atmosphere.			
[RD.26]	https://iridl.ldeo.columbia.edu/documentation/Models/NMME/CanSIPSv2/technote_cansips-v2_20190703_e.pdf			
[RD.27]	J. S. Kain and J. M. Fritsch. A one-dimensional entraining/detraining plume model and its application in convective parameterization. Journal of the Atmospheric Sciences, 47(23):2784–2802, 1990.			
[RD.28]	Belair et al., 2005: Boundary Layer and Shallow Cumulus Clouds in a Medium-Range Forecast of a Large-Scale Weather System. Monthly Weather Review, Vol. 133, 1938-1960			
[RD.29]	Hunke, E.C. and Lipscomb, W.H.. 2010. CICE: the Los Alamos sea ice model, documentation and software user's manual, Version 4.1. Los Alamos, NM, Los Alamos National Laboratory.			
[RD.30]	https://www.gfdl.noaa.gov/climate-models/			2022-11-28
[RD.31]	https://gmao.gsfc.nasa.gov/GEOS_systems/			2022-11-28
[RD.32]	https://www.cesm.ucar.edu/models/ccsm4.0/			2022-11-28
[RD.33]	https://crudata.uea.ac.uk/cru/data/hrg/v4announcement.htm			2022-11-28
[RD.34]	https://climatedataguide.ucar.edu/climate-data/gpcc-global-precipitation-climatology-centre			2022-11-28
[RD.35]	https://psl.noaa.gov/data/gridded/data.gpcp.html			2022-11-28
[RD.36]	https://www.ecmwf.int/en/forecasts/datasets/reanalysis-datasets/era5			
[RD.37]	https://nasagrace.unl.edu/About.aspx			2022-11-24
[RD.38]	https://earth.esa.int/eogateway/missions/smos/description			2022-11-24
[RD.39]	https://smap.jpl.nasa.gov/			2022-11-29
[RD.40]	Jones, H.G.; Schofield, P. Thermal and other remote sensing of plant stress. Gen. Appl. Plant Physiol. 2008, 34, 19–32			
[RD.41]	Mahajan, S.; Tuteja, N. Cold, salinity and drought stresses: An overview. Arch. Biochem. Biophys. 2005, 444, 139–158.			
[RD.42]	Jones, H.G. Application of Thermal Imaging and Infrared Sensing in Plant Physiology and Ecophysiology. In Advances in Botanical Research; Callow, J.A., Ed.; Elsevier Academic Press: San Diego, CA, USA; London, UK, 2004; Volume 41, pp. 107–163			
[RD.43]	Inoue, Y.; Kimball, B.A.; Jackson, R.D.; Pinter, P.J.; Reginato, R.J. Remote estimation of leaf transpiration rate and stomatal resistance based on infrared thermometry. Agric. For. Meteorol. 1990, 51, 21–33			

Ref.	Title	Code	Version	Date
[RD.44]	Jones, H.G. Use of thermography for quantitative studies of spatial and temporal variation of stomatal conductance over leaf surfaces. Plant Cell Environ. 1999, 22, 1043–1055.			
[RD.45]	Norman, J.M.; Becker, F. Terminology in thermal infrared remote sensing of natural surfaces. Agric. For. Meteorol. 1995, 77, 153–166			
[RD.46]	Khanal, S.; Fulton, J.; Shearer, S. An overview of current and potential applications of thermal remote sensing in precision agriculture. Comput. Electron. Agric. 2017, 139, 22–32			
[RD.47]	Mahlein, A.-K. Present and Future Trends in Plant Disease Detection. Plant Dis. 2016, 100, 1–11			
[RD.48]	Berni, J.; Zarco-Tejada, P.J.; Suarez, L.; Fereres, E. Thermal and Narrowband Multispectral Remote Sensing for Vegetation Monitoring From an Unmanned Aerial Vehicle. IEEE Trans. Geosci. Remote Sens. 2009, 47, 722–738.			
[RD.49]	Zarco-Tejada, P.J.; González-Dugo, V.; Williams, L.E.; Suárez, L.; Berni, J.A.J.; Goldhamer, D.; Fereres, E. A PRI-based water stress index combining structural and chlorophyll effects: Assessment using diurnal narrow-band airborne imagery and the CWSI thermal index. Remote Sens. Environ. 2013, 138, 38–50			
[RD.50]	Ullah, S.; Schlerf, M.; Skidmore, A.K.; Hecker, C. Identifying plant species using mid-wave infrared (2.5–6 µm) and thermal infrared (8–14 µm) emissivity spectra. Remote Sens. Environ. 2012, 118, 95–102			
[RD.51]	Ribeiro da Luz, B.; Crowley, J.K. Spectral reflectance and emissivity features of broad leaf plants: Prospects for remote sensing in the thermal infrared (8.0–14.0 µm). Remote Sens. Environ. 2007, 109, 393–405			
[RD.52]	Ribeiro da Luz, B. Attenuated total reflectance spectroscopy of plant leaves: a tool for ecological and botanical studies. New Phytol. 2006, 172, 305–318.			
[RD.53]	Ullah, S.; Skidmore, A.K.; Groen, T.A.; Schlerf, M. Evaluation of three proposed indices for the retrieval of leaf water content from the mid-wave infrared (2–6m) spectra. Agric. For. Meteorol. 2013, 171–172, 65–71			
[RD.54]	Norman, J.M.; Kustas,W.P.; Humes, K.S. Source approach for estimating soil and vegetation energy fluxes in observations of directional radiometric surface temperature. Agric. For. Meteorol. 1995, 77, 263–293			
[RD.55]	Nielsen, S.N. Thermodynamic constraints of life as downward causation in ecosystems. Cybern. Hum. Knowing, 2009, 16, 27–49			
[RD.56]	Koetz, B.; Berger, M.; Blommaert, J.; Del Bello, U.; Drusch, M.; Duca, R.; Gascon, F.; Ghent, D.; Hoogeveen, J.; Hook, S.; et al. Copernicus High Spatio-Temporal Resolution Land Surface Temperature Mission: Mission Requirements Document.			
[RD.57]	Stavros, E.N.; Schimel, D.; Pavlick, R.; Serbin, S.; Swann, A.; Duncanson, L.; Fisher, J.B.; Fassnacht, F.; Ustin, S.; Dubayah, R.; et al. ISS observations offer insights into plant function. Nat. Publ. Gr. 2017, 1, 1–4			
[RD.58]	Gerhards, M., Schlerf, M., Mallick, K., Udelhoven, T., 2019. Challenges and future perspectives of multi-/hyperspectral thermal infrared remote sensing for crop. Remote Sensing. 1240, 11(10).			
[RD.59]	Anderson, M., Yang, Y., Xue, J., Knipper, K., Yang, Y., Gao, F., Hain, C., Kustas, W., Cawse-Nicholson, K., Hulley, G., Fisher, J., Alfieri, J., Meyers, T., Prueger, J., Baldocchi, D., Rey-Sanchez, C., 2021. Interoperability of ECOSTRESS and Landsat for mapping evapotranspiration time series at sub-field scales. Remote Sensing of Environment, 252, 112189			
[RD.60]	Bellvert, J., Jofre-Ĉekalović, C., Pelechá, A., Mata, M., Nieto, H. 2020. Feasibility of using the two-source energy balance model (TSEB) with Sentinel-2 and Sentinel-3 images to analyze the spatio-temporal variability of vine water status in a vineyard. Remote Sensing, 12(14). 10.3390/rs12142299			
[RD.61]	Hu, T., Mallick, K., Hulley, G., Perez, L., Frank, M., Schlerf, M., Hitzelberger, P., Didry, Y., Szantoi, Z., Alonso, I., Hook, S., 2022, Continental-scale evaluation of three ECOSTRESS land surface temperature products over Europe and Africa : Temperature-based validation and cross-satellite comparison. Remote Sensing of Environment, 282(113296)			
[RD.62]	García-Gutiérrez, V., Stöckle, C., Gil, P., Meza, F., 2021. Evaluation of Penman-Monteith model based on Sentinel-2 data for the estimation of actual evapotranspiration in vineyards. Remote Sensing, 1-26, 13(3)			
[RD.63]	Salgado, R., Mateos, L. 2021. Evaluation of different methods of estimating ET for the performance assessment of irrigation schemes. Agricultural Water Management. 243 (106450)			

Ref.	Title	Code	Version	Date
[RD.64]	Ciezkowski, W., Szporak-Wasilewska, S., Kleniewska, M., Jóźwiak, J., Gnatowski, T., Dabrowski, P., Góraj, M., SzatyLowicz, J., Ignar, S., Chormański, J., 2020. Remotely sensed land surface temperature-based water stress index for wetland habitats. Remote Sensing, 12(4)			
[RD.65]	Kogan, F.N., 1995: Droughts of the late 1980s in the United States as derived from NOAA polar-orbiting satellite data. Bulletin of the American Meteorology Society, 76(5)			
[RD.66]	Tarpley, J.D., S.R. Schneider and R.L. Money, 1984: Global vegetation indices from the NOAA-7 meteorological satellite. Journal of Climate and Applied Meteorology, 23:491–494			
[RD.67]	Peters, Albert J. et al. "Drought Monitoring with NDVI-Based Standardized Vegetation Index." Photogrammetric Engineering and Remote Sensing 68 (2002): 71-75			
[RD.68]	Williams, R.E. (1946). Ann. Bot., 10: 41-71.			
[RD.69]	Turner, D.P.; Cohen, W.B.; Kennedy, R.E.; Fassnacht, K.S.; Briggs, J.M. Relationships between leaf area index and Landsat TM spectral vegetation indices across three temperate zone sites. Remote Sens. Environ. 1999, 70, 52-68			
[RD.70]	Sellers, P.J.; Berry, J.A.; Collatz, G.J.; Field, C.B.; Hall, F.G. Canopy reflectance, photosynthesis, and transpiration, III. A reanalysis using improved leaf models and a new canopy integration scheme. Remote Sens. Environ. 1992, 42, 187–216.			
[RD.71]	Peng, J.; Muller, J.-P.; Blessing, S.; Giering, R.; Danne, O.; Gobron, N.; Kharbouche, S.; Ludwig, R.; Müller, B.; Leng, G.; You, Q.; Duan, Z.; Dadson, S. Can We Use Satellite-Based FAPAR to Detect Drought? Sensors 2019, 19, 3662			
[RD.72]	Liu, H. Q., & Huete, A. (1995). A feedback based modification of the NDVI to minimize canopy background and atmospheric noise. IEEE Transactions on Geoscience and Remote Sensing, 33, 457−465			
[RD.73]	Huete, A.R (August 1988). "A soil-adjusted vegetation index (SAVI)". Remote Sensing of Environment. 25 (3): 295–309			
[RD.74]	Anderson, M.C., C. Hain, B. Wardlow, A. Pimstein, J.R. Mecikalski and W.P. Kustas, 2011: Evaluation of drought indices based on thermal remote sensing of evapotranspiration over the continental United States. Journal of Climate, 24(8): 2025–2044			
[RD.75]	Roujean, J.L., M. Leroy and P.Y. Dechamps, (1992). A bidirectional reflectance model of the earth's surface for the correction of remote sensing data. Journal of Geophysical Research, 97 (D18), pp. 20455-20468.			
[RD.76]	Bergman, K.H., P. Sabol and D. Miskus, 1988: Experimental Indices for Monitoring Global Drought Conditions. Proceedings of 13th Annual Climate Diagnostics Workshop, United States Department of Commerce, Cambridge, MA.			
[RD.77]	de Roo, A., Wesseling C. and W. van Deursen. 2000. Physically based river basin modelling within a GIS: the LISFLOOD model, Hydrol. Process. 14, 1981–1992.			
[RD.78]	Wan, Z. and Z.-L. Li, Z. 1997. A physics-based algorithm for retrieving land-surface emissivity and temperature from EOS/MODIS data. IEEE Trans. Geosci. Remote Sens. 35, 980-996.			
[RD.79]	Liu, Y.Y., Dorigo, W.A., Parinussa, R.M., de Jeu, R.A.M., Wagner, W., McCabe, M.F., Evans, J.P.and A.I.J.M. van Dijk. 2012. Trend-preserving blending of passive and active microwave soil moisture retrievals. Remote Sens. Environ. 123, 280-297.			
[RD.80]	Cammalleri, C., Vogt, J.V., Bisselink, B. and A. de Roo. 2017. Comparing soil moisture anomalies from multiple independent sources over different regions across the globe. Hydrol. Earth Syst. Sci. 21, 6329-6343			
[RD.81]	S. K. McFEETERS (1996) The use of the Normalized Difference Water Index (NDWI) in the delineation of open water features, International Journal of Remote Sensing, 17:7, 1425-1432,			
[RD.82]	Kogan, F.N., 1995: Application of vegetation index and brightness temperature for drought detection. Advances in Space Research, 15(11): 91–100.			

Ref.	Title	Code	Version	Date
[RD.83]	Kogan, F.N., 1990: Remote sensing of weather impacts on vegetation in non-homogeneous areas. International Journal of Remote Sensing, 11: 1405–1419.			
[RD.84]	McKee, T. B., N. J. Doesken, and J. Kleist, 1993: The relationship of drought frequency and duration of time scales. Eighth Conference on Applied Climatology, American Meteorological Society, Jan17-23, 1993, Anaheim CA, pp.179-186			
[RD.85]	Edwards, D. C., and T. B. McKee, 1997: Characteristics of 20th century drought in the United States at multiple time scales. Climatology Report No. 97-2, Colorado State Univ., Ft. Collins, CO			
[RD.86]	https://public.wmo.int/en/resources/library/standardized-precipitation-index-user-guide			
[RD.87]	Vicente-Serrano, S. M., Beguería, S., & López-Moreno, J. I. (2010). A Multiscalar Drought Index Sensitive to Global Warming: The Standardized Precipitation Evapotranspiration Index, Journal of Climate, 23(7), 1696-1718.			
[RD.88]	https://fews.net/			2022-12-01
[RD.89]	https://edo.jrc.ec.europa.eu/			2022-12-15
[RD.90]	Cammalleri, C., Arias-Muñoz, C., Barbosa, P., de Jager, A., Magni, D., Masante, D., Mazzeschi, M., McCormick, N., Naumann, G., Spinoni, J., and Vogt, J.: A revision of the Combined Drought Indicator (CDI) used in the European Drought Observatory (EDO), Nat. Hazards Earth Syst. Sci., 21, 481–495,			
[RD.91]	https://edo.jrc.ec.europa.eu/gdo/			2022-12-15
[RD.92]	https://droughtwatch.icpac.net/			2022-12-15
[RD.93]	https://droughtmonitor.unl.edu/			2022-12-01
[RD.94]	https://www.dws.gov.za/niwis2/			2022-12-01
[RD.95]	https://www.arc.agric.za/arc-iscw/Newsletter%20Library/UMLINDI_2022-01,%20January%202022.pdf			2022-12-01
[RD.96]	https://wapor.apps.fao.org/home/			2022-12-01

3. DOCUMENT CONTENT

3.1. CONCEPT AND FRAMEWORK

This chapter introduces the concept of drought monitoring and its relation to agriculture, food security and climate change as well as the agroeconomic systems in Africa and particularly South Africa. It also introduces early warning systems and their components.

3.1.1. FOOD SECURITY, AGRICULTURE, WATER AND CLIMATE CHANGE RELATIONS

According to the Committee on World Food Security of the United Nations, food security is the condition of all people at all times having physical, social, and economic access to sufficient quantities of food that is safe, nourishing, and meets their dietary requirements for an active and healthy life [RD.1]. The principle of food security prioritizes supply to an expanding population of consumers that is either continuous, steady, or not stable, and thus means the removal of variation in production and, consequently, on prices. Later, factors like supply, demand and accessibility were considered because they affect how variable the production process is.

The United States Department of Agriculture (USDA) describes food insecurity as a scenario characterized by "limited or uncertain availability of nutritionally adequate and safe foods or constricted or uncertain ability to acquire acceptable foods in socially acceptable ways [RD.2]." Food security includes a level of resistance to future disruptions or shortages of the essential food supply caused by a variety of risk factors, such as droughts, shipping delays, fuel shortages, unpredictable market circumstances, and wars [RD.3].

Goal 2 of Agenda 2030 states that based on sustainable agriculture, there would be no hunger, food security will be achieved, and nutrition will be clearly sustained by the year 2030 [RD.3]. Food availability, which depends on production, accessibility, which depends on socioeconomic factors, and use, which depends on sociocultural variables, are the three elements of food security. Consequently, to develop a monitoring system for food security, the indicators used should measure the various components' variables [RD.4].

The project proposes to build a drought early warning system that is based on the continuous calculation of a set of indices and indicators. The focus of this work is to identify added-value layers of information that are useful for decision making. The supply of food through production, exchange, and distribution is correlated to its availability. Land ownership and use, soil management, crop selection, breeding, and management, livestock breeding and management, and harvesting are only a few of the variables that affect food production. Temperature and rainfall variations can have an impact on crop productivity [RD.5]. In this sense, climatic water balances (droughts) and climate changes are of special interest.

Drought is a complex phenomenon, which varies every time in terms of its onset, intensity, duration, and geographical coverage. A drought might be meteorological, agricultural, hydrological, or socioeconomic in nature. Its character is primarily determined by its duration: 3 months for meteorological, 6 months for agricultural, 9 months for hydrological, and 12 months or more for socioeconomic. Its severity and length are primarily controlled by the amount of precipitation recorded, the level of potential evapotranspiration, and the spatial distribution of soil types and features of plants [RD.6].

Since 1950, most studies indicate that droughts in Africa have become more frequent, intense, and extensive. The exceptional droughts of 1972–1972, 1983–1984, and 1991–1992 were continental in nature and are unmatched in the records available [RD.7]. South of Angola, Namibia, South Africa, Lesotho, South of Zimbabwe and South of Mozambique, Sahel, and the zone immediately south of it have temperature and precipitation changes that are irreversible or will not return completely to their initial form [RD.8].

Sub-Saharan Africa has the greatest number of water-stressed countries at global scale, since 300 million of Africa's projected 800 million inhabitants reside in a water-stressed environment. Estimations anticipate that by 2030, between 75 and 250 million Africans will live in regions with high water stress, resulting in the displacement of between 24 and 700 million individuals as conditions grow increasingly uninhabitable. Inasmuch as the bulk of Africa continues to rely on an agricultural way of life and 80 to 90 percent of all rural African families rely on generating their own food, water shortage means a decline in food security [RD.9].

3.1.2. SOUTH AFRICA CLIMATE AND AGROECOLOGICAL ZONES

Temperature zones are one of the governing factors in the selection of what crops can be cultivated in what areas. The major climate divisions, as defined for the Global Agroecological Zones (GAEZ) project (FAO/IIASA 2002 [RD.10], represent major latitudinal thermal (or temperature) shifts and are defined as follows:

- **Tropics:** mean monthly temperature adjusted to sea-level greater than 18o C for ALL months
- **Sub-tropics:** mean monthly temperature adjusted to sea-level less than 18 o C for 1 or more months
- **Temperate:** mean monthly temperature adjusted to sea-level less than 5o C for 1 or more months – not applicable for Africa
- **Boreal:** mean monthly temperature adjusted to sea level less than 5o C for all months – not applicable for Africa

In creating the revised AEZ surface for Africa, monthly average minimum and maximum temperature data at a resolution of approximately 1x1km from WorldClim [RD.11] and SRTM30 elevation data also at a resolution of 1x1km [RD.12] were used.

Moisture zones are identified using the length of growing period (LGP) concept which identifies the time with both moisture and temperature are conducive to crop growth. Length of growing period is defined as the period during the year when average temperatures are greater than or equal to 5 °C (Tmean >= 5 °C) and precipitation plus moisture stored in the soil exceed half the potential evapotranspiration (P > 0.5 PET). A normal growing period is defined as one when there is an excess of precipitation over pet (i.e., a humid period). Such a period meets the full evapotranspiration demands of crops and replenishes the moisture definite of the soil profile. An intermediate growing period is defined as one in which precipitation does not normally exceed PET but does for part of the year. No growing period is when temperatures are not conducive to crop growth or P never exceeds PET [RD.13]. The moisture zones were defined using LGP data at a resolution of 10 x 10km [RD.14]. This length of growing period data was provided via personal communication from IIASA and is not yet available for distribution.

The specific moisture zone classes are:

- **Arid:** less than 70 days length of growing period (LGP)
- **Semi-arid:** 70-180 days LGP
- **Sub-humid:** 180-270 days LGP
- **Humid:** >270 days LGP

Highland / Lowland (i.e., Cool / Warm): The major climate and thermal zones provide a broad understanding of the agroecology of Africa but it is equally as important to take into account the effect that changes in elevation have on crops. Certain plants thrive in cooler climates and could possibly be adapted to the highland regions of the tropics but for the most part higher altitudes produce adverse conditions that can restrict agriculture.

This cool/warm distinction requires using daily mean temperature data in conjunction with the start and end dates of the growing season for each cell. The SRTM30 elevation data was first classified into 3 zones as follows:

- **1:** -50 – 800m
- **2:** 800 – 1200m
- **3:** >1200m

Different cut-off values were used for the tropics and subtropics since it takes a greater elevation change for the temperature in the tropics to drop into what is considered a cool zone. For the tropics, areas with greater than 1,200 m elevation were classified as cool; for the subtropics areas with greater than 800m elevation were classified as cool.

The cool/warm assigned classes are:

- 0 = Cold/Boreal (not applicable for Africa)
- 1 = Cool (highland)
- 2 = Warm (lowland)

Final AEZ classification:

The major climates, moisture zones and warm/cool surfaces were combined and each cell was classified into Agroecological Zones classes using the following three-digit combinations:

Climate	**Temperature/elevation**	**Humidity**
Temperate: 1	Warm/Lowland: 1	Arid: 1
Subtropic: 2	Cool/Highland: 2	Semiarid: 2
Tropic: 3	No distinction: 0	Subhumid: 3
Boreal: 4		Humid: 4

This classification of South African agroecology features eleven zones Figure 3-1. A closer look at KwaZulu-Natal, for instance, reveals five distinct agroecological zones. In Limpopo, a comparable number of zones exist.

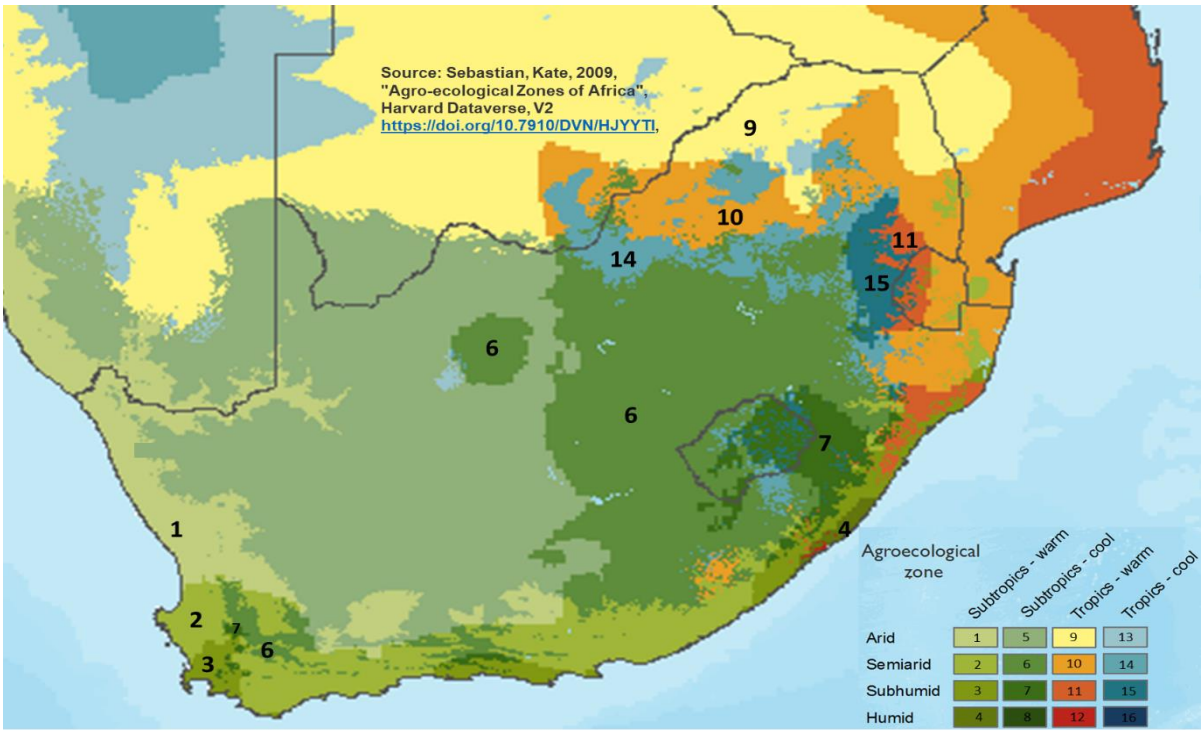

Figure 3-1. South African agroecology zones (source: The International Food Policy Research Institute – Harvard Dataverse agroecological zones (2009)).

Even though the agroecological classification takes precipitation into account to determine a drought event, it is essential to comprehend the regional distribution of precipitation. The images below primarily depict the precipitation for the entire country, ranging from the West (0 – 100 mm/year) to the East (> 1500 mm/year). At the provincial level, a closer look at the province of Limpopo reveals that the annual precipitation ranges from 200 to more than 1,500 millimetres (mm) from south to north. The annual precipitation in Northwest and Free State varies between 200 and 600 millimetres. Consequently, multiple thresholds will be necessary for a single province to identify a state or drought event.

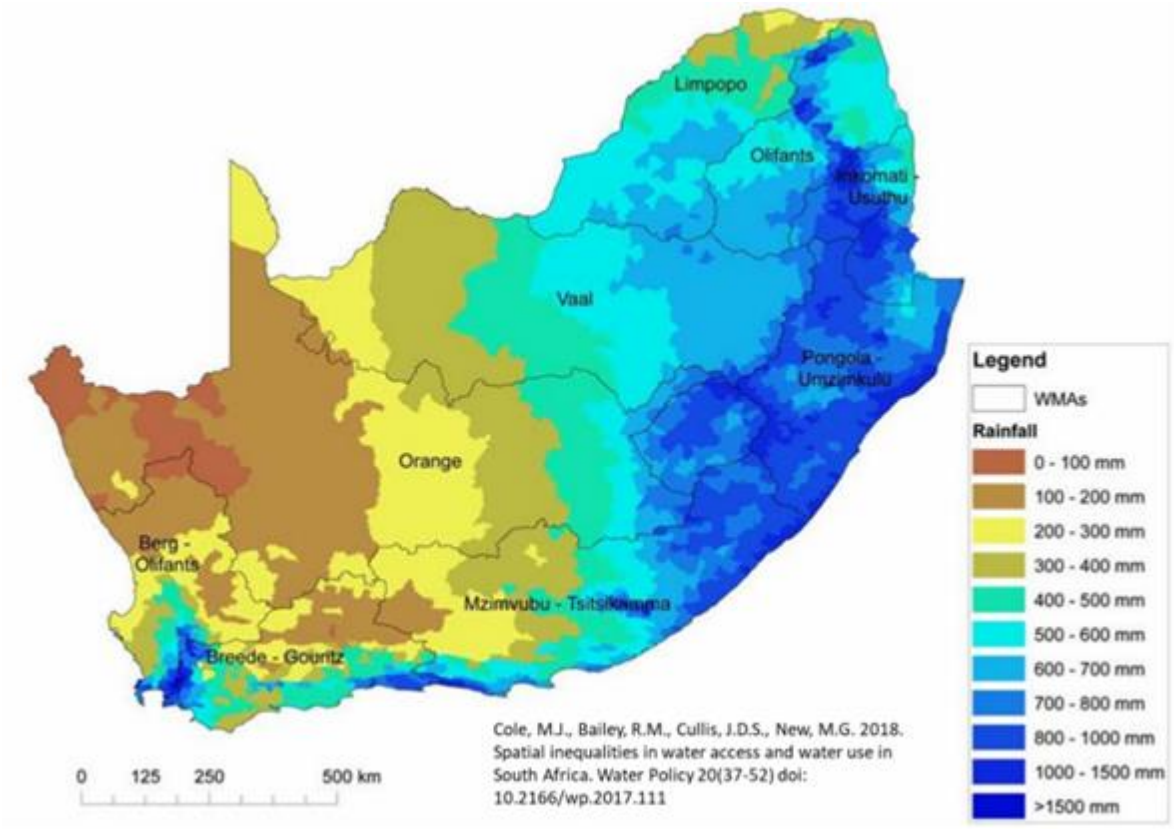

Figure 3-2. South Africa annual precipitation.

Soils are another important variable to consider when determining whether a drought is occurring. Soils play a crucial role in determining the types of crops that can be cultivated and the amount of water required for irrigation to maintain a plantation. In the respective image, the vast diversity of soils in relatively small areas in the East of the country is readily apparent.

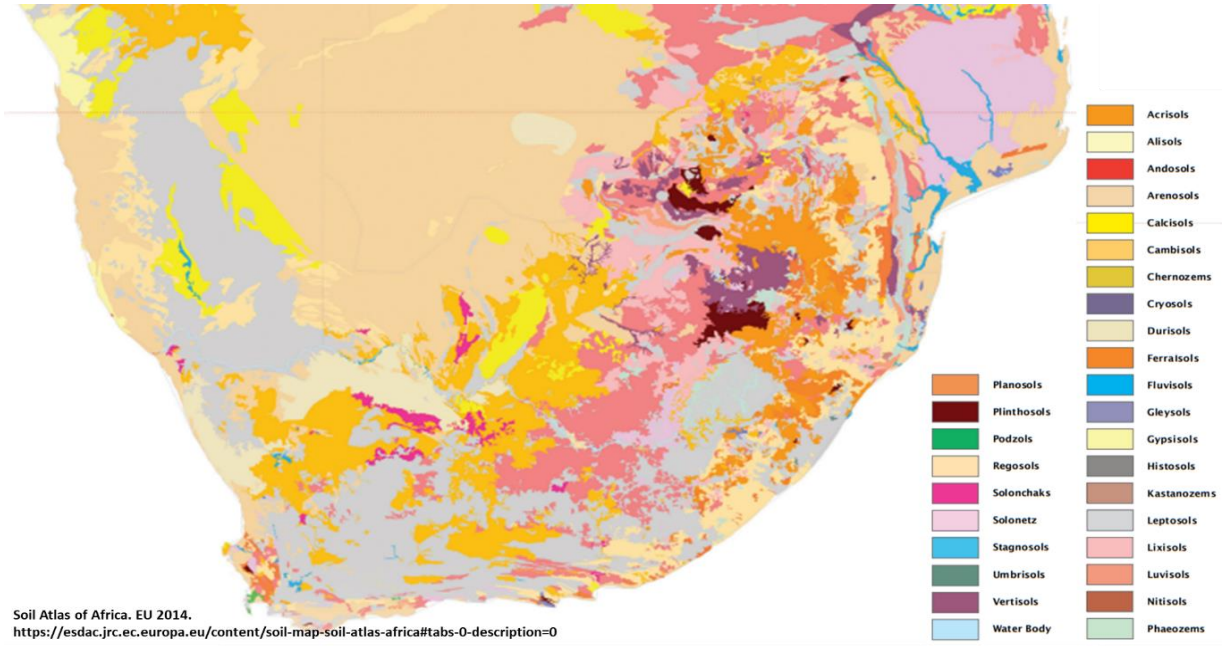

Figure 3-3. South Africa soil map

Precipitation changes in Southern Africa

Several studies have demonstrated that precipitation has increased in some regions of southern Africa over the past few decades. As an illustration, we display the ERA5 and GPCP observations in the IPCC Interactive Atlas [RD.15]. These calculations have a low spatial resolution but, in both instances it serves to identify the regional patrons. The graphs below illustrate the observed trends in mm/day per decade from 1980 to 2015. According to Climate Change Scenario projections and established models accepted by the IPCC, precipitation has been increasing throughout the majority of South Africa. As seen in Figure 3-4 the eastern section of the map, specifically in Eastern Cape and KwaZulu-Natal, the trend is the opposite. The precipitation trend is directly related to the likelihood of drought occurrences and their possible severity.

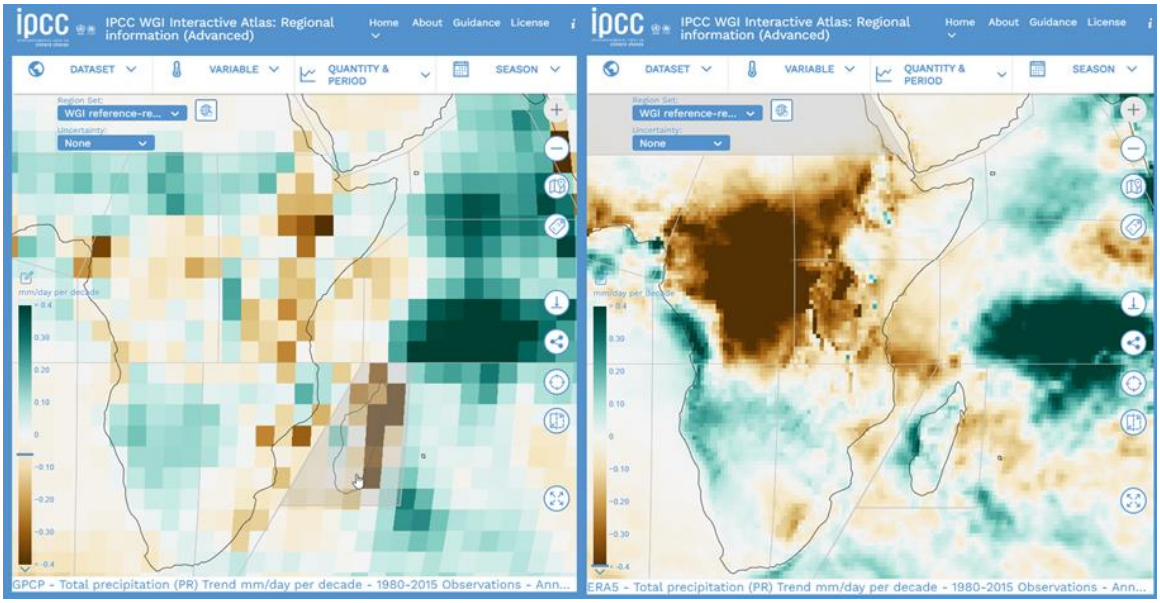

Figure 3-4. GPCP (left) and ERA5 (right) precipitation tends in mm/day from 1980 to 2015.

Moreover, a recent study from Kim et al. 2022 indicates that surface temperature and precipitation undergo irreversible global changes over the course of centuries [RD.19]. In this particular instance, it appears that the changes in the central region of South Africa, where precipitation has increased significantly, are irreversible. The figure below depicts which regions exhibit irreversibility.

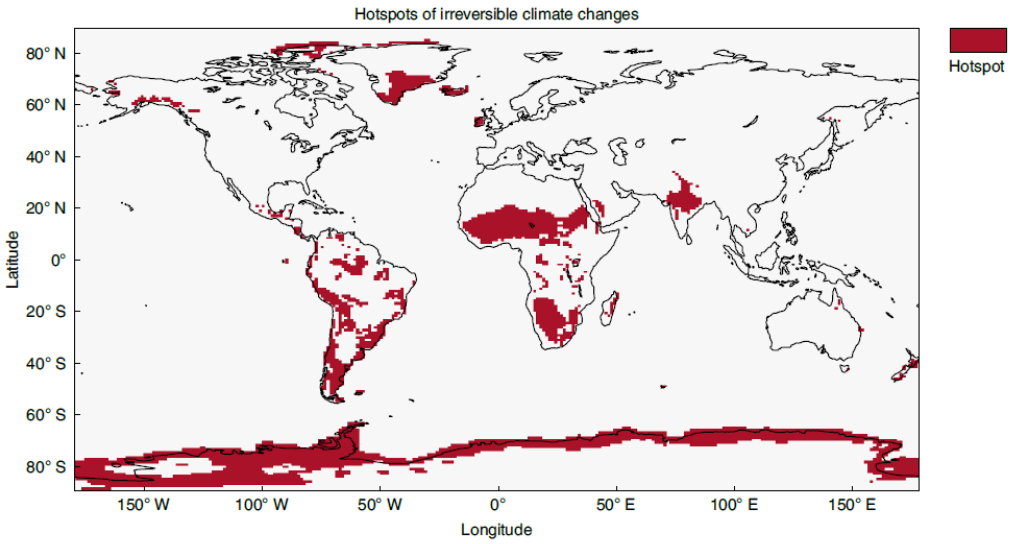

Figure 3-5. Hotspots of irreversible climate change. The identified hotspots for irreversible changes are marked in red. A hotspot is defined as the land area where both surface

temperature and precipitation show an open-loop response (irreversible change) and a large hysteresis area (>50th percentile) to the CO2 forcing.

We conducted a simple analysis of precipitation data for South Africa, Mozambique, Somalia, and Mali from 2001 to 2021 using daily precipitation data from the GPM [RD.17] at a resolution of 10 km. 2004 was the wettest year on the continent during this period. Consequently, this year served as a benchmark. Comparing precipitation from 2001, 2010, 2015, and 2021 to precipitation from 2004 as a baseline we can see a positive trend in precipitation. See figures below arranged from left to right and from top to bottom, respectively.

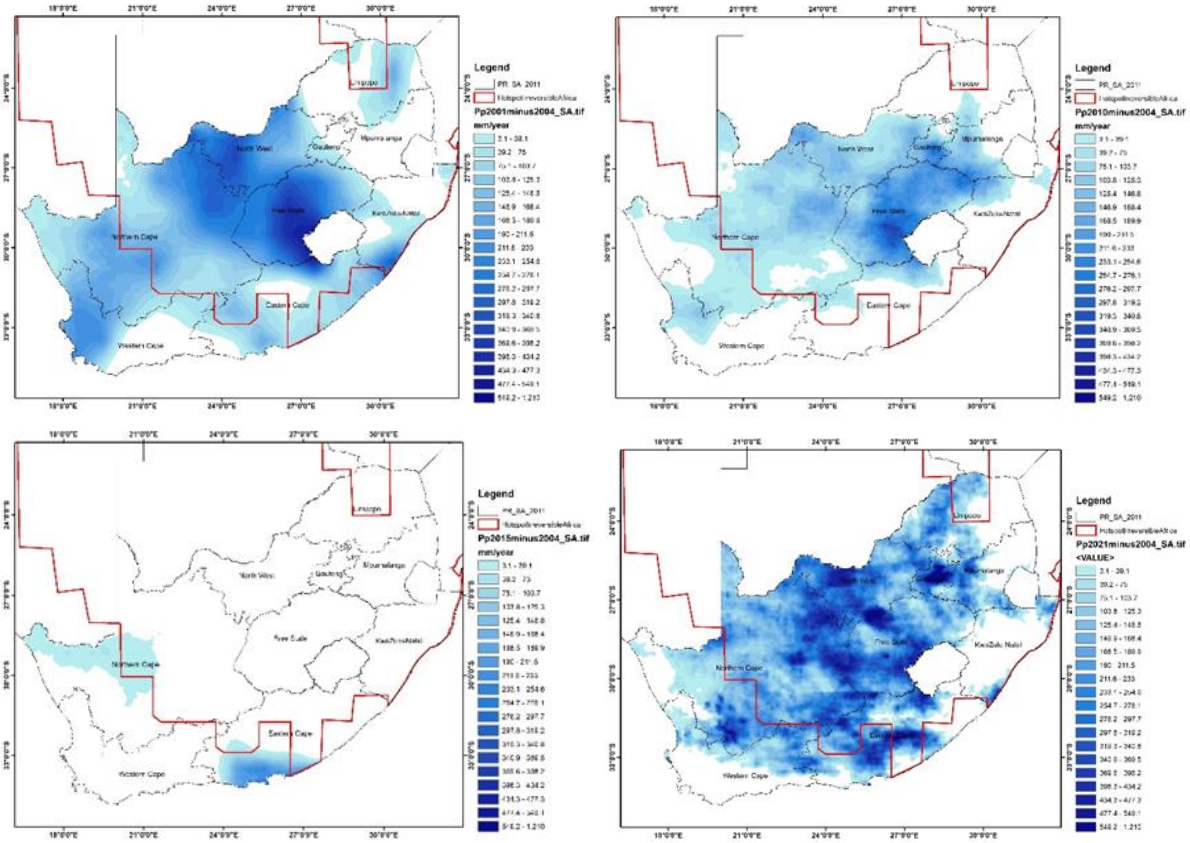

Figure 3-6. Annual precipitation trends for 2001 (upper left), 2010 (upper right), 2015 (lower left) and 2021 (lower right) against a baseline of 2004. The red outline displays the hotspot of irreversible change Source 3IMERGM v6 (Global Precipitation Measurement) precipitation data [RD.18].

As is evident, precipitation levels in 2001, 2010 and 2021 increased significantly from 150 to 300 mm/year on average which could not be reversible. The opposite trend is observed along the country's coast (data not shown – spaces in blank). This analysis considers the past twenty-one years. This trend must be contrasted with the IPCC's CMIP6 projections, which indicate a contrary trend, albeit with very modest changes on the order of less than 10%.

3.1.3. THE PURPOSE OF EARLY WARNING SYSTEMS, THE NATURE OF INFORMATION AND WHAT ARE THE COMPONENTS OF A PERFECT WARNING SYSTEM.

An early warning system is an integrated system that monitors, anticipates, and predicts danger and assesses its risk. Based on this study, the system determines whether to issue a warning or not. The goal is to enable everyone from individuals to governments to minimize catastrophic risks by anticipating

them as the number of recorded disasters has increased by a factor of five, driven in part by human-induced climate change and more extreme weather This was recognized at the COP27: "We must invest equally in adaptation and resilience. That includes the information that allows us to anticipate storms, heatwaves, floods and droughts. To that end, I have called for every person on Earth to be protected by early warning systems within five years, with the priority to support the most vulnerable first [RD.19]]"

Effective early warning systems can have four basic, interdependent parts: (1) knowledge of disaster risk based on systematic data collection and risk assessments; (2) detection, monitoring, analysis, and forecasting of hazards and their likely effects; (3) timely and accurate communication by an authority of actionable warnings and related information on likelihood and impact; and (4) readiness at all levels to respond. For the system to work and give feedback, four parts that depend on each other must be coordinated across sectors and levels. If one part does not work or if they don't work together, the whole system could fail [RD.20]]. This idea must be adjusted depending on the type of risk that will be watched and anticipated for. To show how important the type of threat is, let's look at two completely divergent hydrological events: droughts and floods.

An anomaly in local or regional hydrological patterns is one of the most significant environmental factors that has a significant impact on food security. Each hydrological event can be described initially by the length of time required for its development and occurrence. It can range from hours to months for floods and droughts, respectively. Second, each hydrological event can be defined by its intensity, duration, and frequency once it has occurred. The time frame for its development and recurrence has a direct impact on the type of scientific data that must be collected and the frequency with which it must be processed and examined. In addition, it restricts the period for modelling and predicting its occurrence at certain severity and probability criteria. In addition, this factor will have an effect on the approval procedure for issuing a warning and the communication with the target groups, which vary from people to governments. Consider, for instance, the recent floods in Europe caused by unexpected and intense rain events over the past several years in comparison to the recent floods on the Caribbean and in the Southeast of the United States caused by storms.

Within a few hours to a few days, mesoscale weather models at specialist institutions may be able to predict floods brought on by sudden, intense storms. Therefore, a flood early warning system must collect hourly or sub-hourly data regarding precipitation and concomitant variables such as atmospheric pressure, temperature, and wind speed and direction in very few hours from meteorological stations in order to push the models. The models must identify where precipitation will be released, assess its intensity and potential harm, and then determine who should be notified and how. Once a tropical storm that has the potential to become a hurricane is identified, the models that are applied can anticipate floods caused by hurricanes or storms with several days' notice. In addition to meteorological stations, satellites will also contribute to the period for acquiring pertinent meteorological information. This will enforce the use of data models. The models can create cones with variable probability of occurrence and severity at defined places that anticipate the trajectory of an event. Several towns are alerted, emergency plans are activated and/or upgraded, and authorities at all potential impact sites are notified many days ahead to the occurrence of the catastrophe.

In contrast, a drought event may take several months to develop. The principal hydrological variables that are observed are precipitation, evapotranspiration, and soil moisture. From the perspective of vegetation bioparameters, NDVI, LAI, and fAPAR are significant. Since this phenomenon occurs on a regional scale, remote sensing technology like satellites are the best source of information. These data are collected and assessed every ten days (dekad) and are reviewed months in advance of the start of the growing season. This establishes that the time frames for evaluation, issuing a warning, notification, and responses are significantly longer. In other words, the structure and design of the early warning systems for these three natural phenomena will be actually much different.

The evaluation of an event's severity is essential for determining if a warning should be sent, and it can also limit reaction times. Intensity, frequency, and duration are three characteristics that determine the severity. For the first two flood occurrences caused by a sudden extreme event or a storm/hurricane, the intensity will be determined by the amount of water precipitated per unit of time. The duration

ranges from a few minutes to a number of hours, and the intensity varies every unit of time. In other words, the intensity and duration characterize the histogram of the event, which is typically plotted every 30 minutes. Lastly, the frequency is calculated by the annual chance of occurrence for that specific event (annual maximum precipitation in 24 hours, for example).

The same three characteristics for a drought event are quite different. The intensity is actually quite low or in-existent. The duration is of several weeks and in the past fifty years, drought has gotten more frequent, acute, and widespread, according to most studies. The exceptional droughts in Africa of 1972–1973, 1983–1984, and 1991–1992 were continental in nature and are unmatched in the records available [RD.21]].

3.2. THE TOOLS AVAILABLE

This chapter presents a comprehensive overview of all tools and datasets available for drought monitoring.

3.2.1. HYDROLOGY AND CLIMATE REMOTE SENSED DATA

Remote sensing data includes variables such as temperature, evapotranspiration, and soil moisture. Various satellites and/or sensors can measure these variables. We refer to these as "measurements" and "observations." In order to determine the likelihood of future droughts, it is required to estimate these variables several months in advance starting from the real value of the variable. Therein lies the role of models, which is why models are supported by remotely sensed data.

CLIMATE AND WEATHER MODELS: SEASONAL AND SYNOPTIC TIME FRAMEWORKS

The models required for monitoring and forecasting drought events can be categorized into two types: weather and climate models. Although each type of model has an intrinsic uncertainty, the uncertainties between the two types of models are distinct.

Weather models are used to forecast daily changes in the weather, or to predict what will occur at a certain location and time in the near future, often five to seven days in advance. Because the atmosphere is an inherently chaotic system, model-based weather forecasts are typically less accurate beyond a week. Due to the dynamic nature of the atmosphere, little changes in actual circumstances, which are entered into the model on a regular basis, can result in radically different weather forecasts for the next week.

In contrast, **climate models** do not attempt to predict what will occur at a certain location and time. Therefore, they are unable to give a forecast for, say, March 13, 2053, or even for today. Instead, climate models are used to predict how average circumstances will change, i.e., whether if it will be on average warmer, cooler, wetter, or drier. This information is required to plan for water shortages, more frequent fires, and any other potential local implications of global climate change. Nevertheless, long-term projections (e.g. March, 2053) of water resources are challenging for authorities in terms of planning reservoir operations in lakes or dams given that their immediate concerns are related to the present and near future (5-10 years) water supply and demand.

Using a suite or "ensemble" of climate models can help to improve the clarity of the picture. One model may predict a 3.3 °C change over the next fifty years. Someone else might say 2.7 °C. By employing two, four, six, ten, or fifteen of these models – each of which uses somewhat different methodologies to depict atmospheric processes – we can begin to home in on the expected temperature change, precipitation change, or other variable under consideration. Alternately, an ensemble may be comprised of the same model run several times from a different starting point (for example, using 1990 conditions or 2010 conditions) — this will result in simulations of the future that are slightly different but realistic. For instance, NOAA forecasts that indicate wetter or drier precipitation levels or warmer or cooler than

average temperatures for the upcoming season are mostly based on a single model's ensemble of future possibilities [RD.22].

ECMWF forecasts

ECMWF offers global forecasts, climate reanalysis, and particular datasets tailored to meet the needs of a variety of users. These are accessible through the Internet, point-to-point transmission, data servers, and broadcasting. The operational forecasts of the ECMWF seek to predict how the weather is likely to change. To achieve this, the Centre generates a collection of predictions. Individually, they are exhaustive descriptions of the weather's progression. They collectively represent the probability of a variety of future weather conditions [RD.23].

Monitoring: The purpose of monitoring is to provide statistical data on the quality and availability of the various ECMWF-monitored observing system components. The major objective of the monitoring findings is to maximize the use of observations inside the ECMWF data assimilation systems. The bulk of items undergo daily updates. ECMWF's data assimilation system has access to six-hourly data coverage of observations from this system. The technology utilizes both remote sensing data and regular on-site data. The observations of fourteen satellites are integrated into the ECMWF system. [RD.24]:

The ECMWF system incorporates the following in-situ measurements. Daily updates are performed on specified geographical maps and time series statistics [RD.24]:

- Temperature
- Wind speed
- Surface pressure
- Surface wind speed
- Ground Based GPS
- SYNOP 2M Temperature
- SYNOP snow

Below is a list of monitoring statistics for observations utilized by the ECMWF's ocean data assimilation system. The statistical maps are revised once per week [RD.24]:

- Potential temperature
- Salinity
- Sea level anomaly
- Sea ice concentration

NMME forecasts for the international regions - Regionalized NMME Description:

These models are run on monthly and seasonal (3 months) time steps. The webpage for the regionalized North American Multi-Model Ensemble (NMME) forecasts has been implemented to enable National Meteorological Services (NMSs) around the globe and the public to quickly access operational seasonal model forecasts for specific areas of interest.

The NMME models include:

- The Climate Forecast System Version 2 (CFSv2) produced by the NOAA National Centers for Environmental Prediction (NCEP) is a fully coupled model representing the interaction between the Earth's oceans, land and atmosphere. The four-times-daily, 9-month control runs, consist of all 6-hourly forecasts, and the monthly means and variable time-series (all variables). The CFSv2 outputs include: 2-D Energetics; 2-D Surface and Radiative Fluxes; 3-D Pressure Level Data; 3-D Isentropic Level Data; 3-D Ocean Data; Low-resolution output; Dumps; and High- and Low-resolution Initial Conditions. The monthly CDAS variable timeseries includes all

variables. The CFSv2 period of record begins on April 1st 2011 and continues onwards. CFS output is in GRIB-2 file format [RD.25].

- Two versions of the Canadian models CanCM4i (CMC1) and GEM-NEMO (CMC2), CanCM4i, like CanCM4, couples CCCma's fourth-generation atmospheric model CanAM4 to CCCma's CanOM4 ocean component. Atmospheric horizontal resolution is T63, corresponding to a 128x64 Gaussian grid, with 35 vertical levels and a top at 1 hPa. The 256x192 grid of CanOM4 provides horizontal resolution of approximately 1.4 degrees in longitude and 0.94 degrees in latitude, with 40 vertical levels. Version 2.7 of the CLASS land surface scheme and a single-category, cavitating-fluid sea ice model are employed, both formulated on the atmospheric model grid [RD.26]. GEM-NEMO, developed at the Recherche en Prévision Numérique (RPN), is a fully coupled model with the atmospheric component of GEM and the ocean component of the Nucleus for European Modelling of the Ocean (NEMO).
- The GEM version used is 4.8-LTS.13, with a horizontal resolution of 256×128 grid points (about 155 km) evenly spaced on a latitude-longitude grid, and 79 vertical levels with the top at 0.075 hPa. The land scheme is ISBA, where each grid point is assumed to be independent (no horizontal exchange). The atmospheric deep convection parameterization scheme of Kain-Fritsch [RD.27] is used. The Kuotransient scheme [RD.28] is applied for shallow convections. The model allows for vegetation and ozone seasonal evolutions during the integration. The evolution of anthropogenic radiative forcings are treated simply through specification of equivalent CO2 concentrations with a linear trend. The GEM model is integrated with a time step of one hour. Among the 10 ensemble members in both the forecast and the reforecast, implicit surface flux is used in members 1-5 and explicit surface flux is applied in members 6-10.

- The ocean model NEMO is NEMO 3.6 ORCA 1 with a horizontal resolution of 1°×1° (1/3 degree meridionally near the equator) and 50 vertical levels. The CICE 4.0 (Community of Ice CodE, [RD.29] model is used for the sea-ice component with five ice categories. The NEMO model is run with a 30-minute time step. GEM and NEMO are coupled once an hour through the GOSSIP coupler. No flux corrections are employed in the coupled model [RD.26]].
- NOAA's Geophysical Fluid Dynamic (GFDL),

  GFDL's CM4 consists of AM4 atmosphere at approximately 1o resolution with 33 levels and sufficient chemistry to simulate aerosols (including aerosol indirect effect) from precursor emissions; OM4 MOM6-based ocean at 1/4o resolution with 75 levels using hybrid pressure/isopycnal vertical coordinate; SIS2 sea ice with radiative transfer and C-grid dynamics for compatibility with MOM6; and LM4 land model with dynamic vegetation [RD.31].
- NOAA's Geophysical Fluid Dynamic (GFDL-FLOR),

  The GFDL Forecast-oriented Low Ocean Resolution version of CM2.5 (FLOR) model is a descendent of the CM2.5 model and CM2.1 model. The FLOR model incorporates the higher horizontal resolution in the atmosphere and land, higher vertical resolution in the atmosphere, and significantly improved land model (LM3) from CM2.5. The FLOR model also uses the relatively low-resolution ocean and sea ice components of CM2.1. These choices create a coupled model that is relatively computationally efficient but can be used to address problems of regional climate and extremes [RD.30]].

- National Aeronautics and Space Administration (NASA-GEOS5v2), The Goddard Earth Observing System (GEOS) model consists of a group of model components that can be connected in a flexible manner in order to address questions related to different aspects of Earth Science. GEOS model development adheres to the modular architecture of the Earth System Modelling Framework (ESMF). This modular structure simplifies the management of both the model code and the model configurations, to enable progress with forefront applications of coupled processes in the Earth System. GMAO's work with GEOS spans a large range of space and time scales and encompasses the representation of dynamical, physical, chemical and biological processes [RD.31]

Seasonal forecasts maps are displayed in Multi-Season mode and in Multi-Model mode for all the regions of the world. The Data Downloads tab provides users with access to the seasonal forecast data in binary format and in Climate Predictability (CPT) format for further tailoring of the seasonal forecasts.

RAINFALL ESTIMATES

Global Precipitation Measurement (GPM) – Constant production of measured data every 30 min since June 2000.

The Global Precipitation Measurement (GPM) mission is an international network of satellites that provide next-generation global observations of rain and snow. Building upon the success of the Tropical Rainfall Measuring Mission (TRMM), the GPM concept centers on the deployment of a "Core Observatory" satellite carrying an advanced radar / radiometer system to measure precipitation from space and serve as a reference standard to unify precipitation measurements from a constellation of research and operational satellites. Through improved measurements of precipitation globally, the GPM mission is helping to advance our understanding of Earth's water and energy cycles, improve forecasting of extreme events that cause natural hazards and disasters, and extend current capabilities in using accurate and timely information of precipitation to directly benefit society. GPM, initiated by NASA and the Japan Aerospace Exploration Agency (JAXA) as a global successor to TRMM, comprises a consortium of international space agencies, including the Centre National d'Études Spatiales (CNES), the Indian Space Research Organization (ISRO), the National Oceanic and Atmospheric Administration (NOAA), the European Organization for the Exploitation of Meteorological Satellites (EUMETSAT), and others.

IMERG Final Run: Research-quality gridded global multi-satellite precipitation estimates with quasi-Lagrangian time interpolation, gauge data, and climatological adjustment [RD.35]. This algorithm is intended to intercalibrate, merge, and interpolate "all" satellite microwave precipitation estimates, together with microwave-calibrated infrared (IR) satellite estimates, precipitation gauge analyses, and potentially other precipitation estimators at fine time and space scales for the TRMM and GPM eras over the entire globe. The system is run several times for each observation time, first giving a quick estimate (IMERG Early Run) and successively providing better estimates as more data arrive (IMERG Late Run). The final step uses monthly gauge data to create research-level products (IMERG Final Run).

The main differences between the IMERG Early and Late Run are:

- The half-hourly Final Run product uses a month-to-month adjustment to the monthly Final Run product, which combines the multi-satellite data for the month with GPCC gauge analysis. The adjustment within the month in each half hour is a ratio multiplier that's fixed for the month, but spatially varying.
- The Late Run is computed about 14 hours after observation time, so sometimes a microwave overpass is not delivered in time for the Late Run, but subsequently comes in and can be used in the Final. This would affect both the half hour in which the overpass occurs, and (potentially) morphed values in nearby half hours.

We always advise people to use the Final Run for research unless their application will require the use of Early or Late data due to latency. In such a case, the application should be developed using the long record of the Early or Late, as appropriate. The vast majority of grid boxes have fairly similar Late and Final values over ocean, and to a lesser extent over land. Extreme value statistics are more sensitive to these details; medians, means, and root-mean square difference are less sensitive.

CRU TS monthly high-resolution gridded climate dataset (CRU TS) – 1901 - 2018

A new paper describing version 4 of the CRU TS multivariate climate data set is published in Nature's Scientific Data [RD.36]. CRU TS is one of the most widely used observed climate datasets and is produced by the UK's National Centre for Atmospheric Science (NCAS) at the University of East Anglia's Climatic Research Unit (CRU).

CRU TS provides monthly data on a 0.5° x 0.5° grid covering land surfaces (except Antarctica) from 1901 to 2018 (the next release, which is imminent, will extend this to 2019). There are ten variables, all based on near-surface measurements: temperature (mean, minimum, maximum and diurnal range), precipitation (total, also rain day counts), humidity (as vapour pressure), frost day counts, cloud cover,

and potential evapotranspiration. CRU TS has been produced and shared openly to facilitate research and analysis in all areas related to climate and climate change since the first version was released in 2000. Version 4 is the first major update since version 3 was published in 2013.

Version 4 features an improved interpolation process, which delivers full traceability back to station measurements. The station measurements of temperature and precipitation are provided as well as the gridded dataset and national averages for each country. Cross-validation was performed at a station level, and the results can be examined in the paper as a guide to the accuracy of the interpolation. The overall process is always being refined and improved; an approach made possible by NCAS funding as part of the NCAS Long-Term Global Change theme.

CRU TS is used in many different contexts, from analysis of climate variability/change and evaluation of climate models, through to the many sectors that are impacted by climate such as hydrology, insurance and civil engineering. Although it is not possible to measure the full extent of its use due to inconsistent (and occasionally absent) citations, Google Scholar citations of the scientific papers describing the first three versions provide a guide (>2300 for version 1, >4200 for version 2, and >3900 for version 3) [RD.37].

Global Precipitation Climatology Centre (GPCC) 1901 – 2010

The GPCC offers gridded gauge-analysis products made from station data that has undergone quality control. There are two products for studying climate variability and trends: (a) the VASClimO50-Year Data Set, which is for studies of climate variability and trend, and (b) the Full Data Reanalysis Product (1901–2010), which is advised for studies of global and regional water balances, calibration/validation of remote sensing-based rainfall estimates, and verification of numerical models. A systematic gauge measurement error bias correction is not applied to the products. The number of gauges utilized on the grid and estimates for that mistake are also provided by the GPCC [RD.37]].

- 64,400 or so stations are in use, and the gauge network goes beyond the GHCN
- A significant source of inhomogeneity can be the fluctuating number of stations non each grid throughout time.
- While climate products are not often updated, monitoring items are.

The Global Precipitation Climatology Project (GPCP) Monthly Precipitation Climate Data Record (CDR) – 1979 – present

The GPCP Monthly product provides a consistent analysis of global precipitation based on the integration of numerous satellite data sets over land and water and a gauge analysis of land precipitation. Since 1979, data from rain gauge stations, satellites, and sounding measurements have been used to estimate monthly precipitation on a 2.5-degree worldwide grid. The meticulous combining of satellite-based rainfall estimates gives the most comprehensive analysis of rainfall to date over the world's oceans and adds important spatial depth to analyses of rainfall over land. In addition to the combining of these data sets, the GPCP outputs also provide estimates of the uncertainties in the rainfall analysis. Current version number is 2.3. There may be interim data at the end of the dataset. There is a netcdf attribute that contains the interim data for the first month [RD.38].

SOIL MOISTURE

GRACE-based root zone soil moisture and surface soil moisture

Scientists at NASA’s Goddard Space Flight Center generate groundwater and soil moisture drought indicators each week. They are based on terrestrial water storage observations derived from GRACE-FO satellite data and integrated with other observations, using a sophisticated numerical model of land surface water and energy processes. The drought indicators describe current wet or dry conditions, expressed as a percentile showing the probability of occurrence for that particular location and time of

year, with lower values (warm colours) meaning dryer than normal, and higher values (blues) meaning wetter than normal. These are provided as both images and binary data files.

The Contiguous U.S. (CONUS) indicators are generated at 0.125 degree, while the Global Land indicators are at 0.25 degree resolution. NASA's Gravity Recovery and Climate Experiment satellites were the only ones capable of measuring fluctuations in water stored at all levels above and within the ground surface (terrestrial water storage). The GRACE mission concluded in 2017, however the GRACE-FO mission, which started on May 22, 2018, is already extending the data record. The spatial (>150,000 km^2) and temporal (monthly with a substantial time lag) resolutions of the GRACE and GRACE-FO fields restrict their direct use for drought assessment. NASA/GSFC scientists integrate GRACE and GRACE-FO data with other ground- and space-based meteorological observations (precipitation, solar radiation, etc.) within the Catchment Land Surface Model, employing Ensemble Kalman smoother type data assimilation, in order to increase the resolution, eliminate the time lag, and isolate groundwater and other components from total terrestrial water storage. The generated fields of soil moisture and groundwater storage fluctuations are then utilized to construct drought indicators based on the Catchment model's simulation of the cumulative distribution function of wetness conditions from 1948 to 2014. Houborg et al. (2012) provide comprehensive information on the creation of U.S. GRACE-based drought indicator products. Li et al. (2019) present information on the assimilation of global GRACE and GRACE-FO data and the production of drought indicator products. Getirana et al. (2020) provide information on the creation of drought/wetness forecast products for the CONUS [RD.37].

Soil Moisture and Ocean Salinity (SMOS)

The SMOS mission is a direct response to the existing shortage of worldwide measurements of soil moisture and ocean salinity, which are essential for advancing our understanding of the water cycle and improving weather, extreme-event, and seasonal-climate forecasts. Variation in soil moisture and ocean salinity is a result of the constant exchange of water between the oceans, atmosphere, and land - the water cycle of the Earth [RD.38]. Variability in soil moisture is mostly determined by varying evaporation and precipitation rates. The estimation of soil moisture at the root zone is crucial for developing short- and medium-term meteorological models, hydrological models, the monitoring of plant growth, and the prediction of disastrous events such as floods.

Obviously, soil moisture is essential for primary production, but it is also inextricably tied to our weather and climate. This is because soil moisture is a crucial factor in regulating the exchange of water and heat energy between the ground and the atmosphere. The terrestrial portion of the water cycle is comprised of precipitation, soil moisture, percolation, runoff, soil evaporation, and plant transpiration. Therefore, there is a direct relationship between soil moisture and atmospheric humidity, as dry soil contributes little or no moisture to the atmosphere, whereas moist soil contributes a great deal. Moreover, because soil moisture is linked to evaporation, it is also significant in regulating the distribution of heat flux from the land to the sky, such that regions with high soil moisture not only increase local atmospheric humidity but also decrease local temperatures [RD.38]. Accuracy of 4% volumetric soil moisture; Spatial resolution 35-50 km; Revisit time 1-3 days.

Soil Moisture Active Passive (SMAP)

The Soil Moisture Active Passive (SMAP) project is an orbiting observatory that measures the water content of the Earth's surface soil. The SMAP radiometer has been performing without defect. Due to the loss of the radar's power source, the radar instrument ceased operation in early 2015, after collecting close to three months' worth of scientific data. The three-year prime mission phase of SMAP was concluded in 2018, and the mission is now in its extended operating phase. The topsoil is the layer in which our food and other vegetation grow and thrive. Indirectly, soil moisture influences us in a variety of ways. During its observations, SMAP will also identify whether the ground in colder regions of the globe is frozen or thawed. Every two to three days, SMAP is meant to measure soil moisture. This enables the observation of global changes on timescales ranging from extreme weather events to recurrent seasonal surveys.

SMAP estimates the amount of water in the top layer of soil everywhere on Earth not covered by water or frozen. It also distinguishes between frozen and thawed ground. It quantifies the quantity of water

found between the minerals, rocky material, and organic particles found in soil everywhere in the world when the earth is not frozen (SMAP measures liquid water in the top layer of ground but is not able to measure the ice.). SMAP will generate global soil moisture maps. These will be utilized by scientists to enhance our comprehension of how water, energy, and carbon fluxes (in their various forms) manage our climate and environment. The water cycle encompasses more than the obvious processes of evaporation from the oceans and land, condensation generating clouds that eventually drop rain or snow (precipitation), and water travelling through the land before returning to the sea. For instance, plants absorb water from the soil in order to develop, but they also "transpire" a portion of it directly into the air.

Water cycle has fewer branches than carbon cycle. It refers to the transport of carbon between and among the atmosphere (air), pedosphere (soil), lithosphere (rock), hydrosphere (surface water: ocean, lakes, and rivers), and cryosphere (frozen regions) of the Earth (all forms and places where ice is found on Earth including sea ice, snow, glaciers, and permafrost). Carbon (in the form of carbon dioxide) is present in the air, dissolved in water, emitted from subsurface sources, and exhaled by all living organisms. There are carbonate minerals on the ocean floor, in mountains, and in the famed White Cliffs of Dover. Carbon is contained underground in petroleum and coal until it is pumped or mined. All these kinds of carbon can cycle through the spheres in diverse ways.

Weather and climate studies will also utilize SMAP data. The soil moisture determines the amount of water that evaporates from the land surface into the atmosphere. Information on soil moisture is essential for comprehending the water and heat energy exchanges between the surface and atmosphere that influence weather and climate. Since April 2015, SMAP data have offered an abundance of information regarding regional and global soil moisture variability. SMAP's frequent and accurate monitoring of soil moisture will enhance the forecasting abilities of weather and climate models [RD.39].

TEMPERATURE

To ensure global water and food security, it is of the utmost importance to identify plant water stress or drought. Consequently, knowledge of crop water status across expansive farming areas can optimize agricultural water use. Water-deficit stress (drought) refers to the physiological reactions of plants generated by a shortage of accessible water caused by either a soil water deficit or a high evaporative demand from the atmosphere. Water stress is one of the most important abiotic stressors that limit plant development, crop yield, and food quality [RD.40]. Before apparent indications of water stress show, plants might be irreparably damaged [RD.41]. Consequently, a pre-symptomatic or pre-visual identification of plant physiological changes might significantly aid in preventing severe crop losses.

Cell turgor and leaf water content are diminished under severe and/or persistent water stress [RD.42]. As a result, stomatal closure reduces the exchange of water vapour between plants and the atmosphere, reducing the evaporative cooling effect and resulting in an increase in plant surface temperature relative to a plant that is not under water stress [RD.43]. Nonetheless, stomata regulate not just plant transpiration but also plant respiration, which prevents CO_2 absorption and fixation. Due to stomatal closure, the photosynthetic rate is lowered, resulting in a decrease in yield. While a decrease in CO_2 uptake owing to stomatal closure reduces the photosynthetic rate, irradiance and absorbed photosynthetically active radiation (fAPAR) remain unchanged. It is well established, based on the leaf energy balance equation, that leaf temperature fluctuates with (evapo-) transpiration rates of the leaves and is, thus, a function of stomatal conductance. Temperature of the leaf has an inverse relationship with transpiration rate. Typically, the leaf temperature of a fully transpiring plant is between 2 and 5 degrees Celsius below the ambient air temperature [RD.44].

Thermal infrared (TIR) multi-/hyperspectral method and conventional solar-reflective (visible, near-, and shortwave infrared reflectance (VNIR - SWIR) hyperspectral remote sensing are the most advanced techniques for detecting agricultural water stress. Since the 1970s, TIR remote sensing (8–14 μm) has been recognized as a “possible” method for early detection of plant water stress. TIR indices offer significant application potential in precision agriculture, particularly in irrigation management, to determine the optimal time, place, and amount of water to apply to reduce the amount of water consumed per unit of yield. In general, emitted light in the TIR contains two intrinsic types of

information: (i) the surface temperature (i.e., "directional radiometric surface temperature"[RD.45] and (ii) the spectral emissivity of the item of interest.

Numerous airborne and satellite TIR sensors have been created and utilized in agriculture due to the huge potential of temperature-based indices for the pre-visual identification of plant reactions to water stress [RD.46]. As a result of their low spatial and temporal resolution, however, satellite sensors are inadequate for precision agriculture applications. Landsat 8 has the best spatial resolution with 100 m, which corresponds to a single field per pixel for most agricultural cultivation systems [RD.47]. Consequently, recent advances in TIR remote sensing from airborne and Unmanned Aerial Vehicles (UAVs) offer the potential to bridge the gap between low-resolution satellite images and small-scale in situ measurements [RD.48]. The bulk of research estimate temperature-based indices for the identification of plant responses to water stress using broadband TIR sensors [RD.49]. Broadband TIR imagers (one spectral band in the wavebands of 7–14 μm) are based on the assumption of a constant emissivity, which does not exist in nature (e.g., 0.97 for vegetation)[RD.50]. However, new hyperspectral TIR imagers offer new methodologies that enable exact spectral emissivity retrieval and, consequently, more accurate surface temperature calculation.

From the emissivity based approach it can be said that: the generalization that vegetation does not generate sufficient spectral features in the TIR for studying plant physiological properties is contingent on a number of factors [RD.51]: (1) General lack of hyperspectral remote sensing instruments (most available setups are based on laboratory equipment); (2) Extremely low and complex spectrum emissivity fluctuations originate from intricate plant physiological and biochemical processes; (3) Airborne or satellite remote sensing TIR sensors with low signal-to-noise ratio (SNR) and low spatial and spectral resolution are incapable of detecting tiny fluctuations in the TIR spectral fingerprint of plants; (4) To extract precise emissivity spectra, atmospheric correction and advanced TES techniques are required.

As opposed to VNIR/SWIR spectra, which are primarily dominated by overtones and combination modes of fundamental vibrations resulting from interactions between solar radiation and leaf contents, TIR spectra are primarily derived from primary absorption bands of biochemical leaf compounds, such as cellulose, and should therefore exhibit higher spectral contrast (e.g., leaf pigments) [RD.52]. Therefore, changes in the emissivity spectra should coincide with changes in the proportions of leaf elements brought on by water stress [RD.53].

The physically based modelling of evapotranspiration (ET) could provide an alternative method not only for the detection of plant responses to water scarcity, but also for the elucidation of plant-pedosphere-atmosphere interactions under environmental stress situations. Estimation of ET by TIR remote sensing is based on surface energy balance (SEB) models. The primary assumption of using land-surface temperature (LST) in a SEB model is, TIR remote sensing can provide direct information of the land-surface moisture status impacting the surface energy fluxes and their partitioning [RD.54].

Current improvements in sensor technology have enabled imaging hyperspectral remote sensing of plants in the TIR spectral domain, allowing for the detection of environmental stressors via spectral emissivity. However, current TIR satellites do not meet the parameters (high SNR, high spectral and spatial resolution) necessary to measure the low spectral contrast emissivity characteristics of plants from space. Consequently, the scaling up of emissivity-based methods for detecting water stress from space is still somewhat limited. In order to better comprehend the relationships between the spectral emissivity characteristics and changes in leaf attributes under environmental stress situations at different remote sensing scales, additional fundamental study is required. The law of thermodynamics states that when a system evolves, its entropy and disorder rise, and it finally reaches equilibrium (i.e., the same temperature) with its surroundings. However, ecosystems can live and thrive while being out of balance with their surroundings, due to irreversible processes that contribute to a continuous increase in entropy and chaos. This appears contradictory, presenting a conundrum.

The assumption that entropy being exported to the environment is essential for reconciling these two seemingly contradicting facts [RD.55]. Thus, an ecosystem can be out of balance with its surroundings

and maintain a lower temperature than its surroundings. The following premise underpins the use of temperature as an indicator of drought stress. A tropical forest would have a lower temperature than a crop plantation, which would have a lower temperature than a savanna, which would have a lower temperature than bare soil under equal environmental conditions. In other words, the more the complexity of an ecosystem, such as a tropical rain forest, the more work it can do and the larger its buffering capacity, which results in a lower temperature than crop plantations or grasslands alone or bare soils.

Latest TIR satellite missions

Due to the lack of multi- and hyperspectral TIR satellites, mission designs such as LSTM (Land-Surface Temperature Monitoring [RD.56] offer very promising perspectives for the use of multi-/hyperspectral TIR for the detection of environmental stresses from space. In 2018, four cutting-edge Earth-observation devices were tested for prospective future satellite-based plant function monitoring aboard the International Space Station (ISS) [RD.57].

The instruments were the Global Ecosystem Dynamics Investigation (GEDI, NASA), the Ecosystem Spaceborne Thermal Radiometer Experiment on Space Station (ECOSTRESS, NASA), the Orbiting Carbon Observatory (OCO-3, NASA), and the Hyperspectral Imager Suite (HISUI, JAXA).

- GEDI carries a LiDAR (Light Detection And Ranging) measuring canopy structural parameters (e.g., height, biomass).
- ECOSTRESS will deliver TIR data items (such as surface temperature and ET).
- OCO-3 measures SIF and HISUI delivers surface reflectance (10 nm spectral resolution) in the VNIR/SWIR.

The data products will be freely accessible and will provide scientists with opportunities to examine the performance and capabilities of such an innovative satellite-based multi-sensor approach to examine plant functioning and the response to environmental stress in a wide variety of ecosystems. Particularly, the ECOSTRESS sensor aboard the International Space Station (ISS) will provide initial insights for future TIR satellite missions.

Thermal infrared (TIR)-based surface energy balance (SEB) modelling has proven to be an efficient method for tracking consumptive water use in agricultural systems at various spatial scales. Land-surface temperature (LST) maps derived from TIR remote sensing provide a helpful proxy measure of the surface moisture condition, constraining latent heat (energy flux) and evapotranspiration (ET; mass flux) estimations from SEB models at the pixel scale. For highest benefit in agricultural water management applications, frequent thermal imaging (4-day revisit) at sub-field (100 m or less) spatial resolution is necessary.

While the current fleet of Landsat satellites (7 and 8) provides the requisite spatial resolution, the 8-day combined revisit can be insufficient to detect quick changes in surface moisture status or crop phenology, especially in regions with persistent cloud cover. Current state-of-the-art thermal infrared sensing satellites deliver either high temporal (e.g., MODIS, AVHRR, or Sentinel-3 with 1–3 days revisit time) but coarse spatial (i.e., 1 km) resolution images or high spatial (e.g., Landsat series, Advanced Spaceborne Thermal Emission and Reflection Radiometer (ASTER) with 100 m) but low temporal (i.e., 16 days) resolution images. Multi-sensor scaling, such as pan-sharpening, or more advanced disaggregation techniques could be one solution (e.g., thermal sharpening or temperature unmixing). The combining of distinct spectral domains in a multisensor method would provide the potential for novel soil–plant–atmosphere continuum discoveries [RD.58].

One of the most recent efforts in this direction was performed when the new ECOsystem Spaceborne Thermal Radiometer Experiment on Space Station (ECOSTRESS) mission - average 4-day return interval and nominal 70-m resolution - was utilized as a platform for enhancing Landsat TIR sampling and researching TIR-based ET mapping mission requirements more generally.

Here, the interoperability of Landsat and ECOSTRESS imaging was evaluated for producing ET image timeseries with high spatial (30 m) and temporal (daily) resolution. A data fusion algorithm was used to combine Landsat and ECOSTRESS ET retrievals at 30 m with daily 500-m retrievals utilizing TIR data from the Moderate Resolution Imaging Spectroradiometer (MODIS) over agricultural sites of interest across the United States. Comparing the combined multi-source dataset to daily flux tower observations gathered within these target domains, the increased value of the combined dataset was assessed. The results highlighted the significance of the more frequent temporal sampling given by ECOSTRESS, particularly in cloud-prone regions. Limiting usage to ECOSTRESS scenes acquired between 9:00 a.m. and 5:00 p.m. and nadir viewing angles 20 degrees produced daily (24-h) ET retrievals of equal quality to the well-established Landsat baseline [RD.59].

One of the biggest constraints of using energy balance models to estimate actual evapotranspiration is the coarse spatial resolution in the thermal infrared (TIR) domain. In this regard, the European Space Agency's (ESA) Sentinel missions have substantially increased the ability to monitor crop characteristics and estimate ET at higher temporal and spatial resolutions.

Sharpening techniques were employed to downscale the Sentinel-3 land surface temperature (LST) from 1 km to 20 m in order to bridge the gap between the coarse-resolution Sentinel-3 thermal and the fine-resolution Sentinel-2 shortwave data.

LST is a crucial piece of information for assessing hydrological conditions in connection to agricultural activities. Despite this, LST is crucial to the estimation of other significant hydrological variables, such as actual and potential evapotranspiration. Water scarcity is one of the most significant issues facing agroecosystems that rely heavily on irrigation, like vineyards. Mapping Evapotranspiration, based on thermal infrared data from Landsat 7 and Landsat 8, with high Resolution and Internalized Calibration (METRIC), and Priestley–Taylor Two Source Model were used as a reference to evaluate the performance of evapotranspiration models (Penman–Monteith–Stewart and Penman–Monteith–Leuning) based on remote sensing data from visible bands of Sentinel-2 [RD.62].

Spectral Indices

NORMALIZED DIFFERENCE VEGETATION INDEX

The Normalized Difference Vegetation Index (NDVI) is a well-established method to quantify vegetation greenness and is useful in understanding vegetation density and assessing changes in plant health captured in a satellite image. NDVI is one of the most common remote sensing indices. Its practical applications are incredibly diverse, including quantifying forest supply, serving as a drought indicator, forecasting fire zones and mapping desertification [RD.65].

Healthy vegetation has a very characteristic spectral reflectance curve which we can benefit from by calculating the difference between two bands – visible red (R) and near-infrared (NIR). NDVI is that difference expressed as a number – ranging from -1 to 1. NDVI is derived from satellite imagery and calculated in accordance with the formula:

$$\text{NDVI} = \frac{(NIR - R)}{(NIR + R)}$$

NDVI defines values from -1.0 to 1.0, where negative values mainly represent clouds, water and snow, and values close to zero primarily depict rocks and bare soil. Very small values (0.1 or less) of the NDVI

function correspond to empty areas of rocks, sand, or snow. Moderate values (from 0.2 to 0.3) represent shrubs and meadows, while large values (from 0.6 to 0.8) indicate temperate and tropical forests [RD.66].

STANDARDIZED VEGETATION INDEX

The Standardized Vegetation Index (SVI) described by Peters et al. 2002, is derived from the NDVI, describes the probability of vegetation condition deviation from "normal", based on calculations from weekly NDVI values. Z-scores of the NDVI distribution are used to estimate the probability of occurrence of the present vegetation condition at a given location relative to the possible range of vegetative vigour, historically. The z score is a deviation from the mean in units of the standard deviation, calculated from the NDVI values for each pixel location for each week for each year [RD.67].

$$Z_{ijk} = \frac{NDVI_{ijk} - \overline{NDVI}_{ij}}{\sigma_{ij}}$$

Z_{ijk} is the z-value for pixel i during week j for year k, $NDVI_{ijk}$ is the weekly NDVI value for pixel i during week j for year k, $NDVI_{ij}$ is the mean NDVI for pixel i during week j over n years, and σij is the standard deviation of pixel i during week j over n years. Z_{ijk} assumes to fit a standard normal distribution, which has mean of zero and standard deviation of 1, denoted as $Z_{ijk} \sim N(0, 1)$. Therefore, the probability density function of Z_{ijk} is given by :

$$SVI = P(Z < Z_{ijk})$$

This per-pixel probability, expressed as the SVI, us ab estimate of the probability of occurrence of the present vegetation condition. The values of the SVI range between greater than zero and less than one. Zero is the baseline condition in which a pixel NDVI value is lower than all possible NDVI values for that week in other years. One is the baseline condition in which the pixel NDVI value for the respective week is higher than all the NDVI values of the same week in other years. Typically, the SVI values are grouped in five classes, which compromises different and consecutive ranges of values, very poor (0 to 0.05), poor (0.05 to 0.25), average (0.25 to 0.75), good (0.75 to 0.95), and very good (0.95 to 1). These classes mimic a normal probability density function, for example a pixel classified as very good indicates that its NDVI value is higher than average, or that vegetation is in very good relative condition, compared to the average during the same week of the year relative to that of other years.

LEAF AREA INDEX

Leaf area index (LAI) quantifies the amount of leaf area in an ecosystem and is a critical variable in processes such as photosynthesis, respiration, and precipitation interception. As a fundamental attribute of global vegetation, LAI has been listed as an essential climate variable by the global climate change research community en is a critical parameter for understanding terrestrial, ecological, hydrological, and biogeochemical processes [RD.68].

$$LAI = \frac{leaf\ area\ (m^2)}{ground\ cover\ (m^2)}$$

LAI can be estimated from remote sensing data using either statistical or physical methods. The statistical methods use the empirical relationship between the LAI and surface reflectance or vegetation indices. The physical methods determine the LAI based on radiative light transfer processes within the canopy. Various retrieval methods, including neural network methods, genetic algorithms, Bayesian networks, and lookup table methods can be used to retrieve LAI. In addition, major global moderate-resolution LAI products, such as Moderate Resolution Imaging Spectroradiometer, GEOV1, GLASS, GLOBMAP, and CCRS have been developed [RD.69].

FRACTION OF ABSORBED PHOTOSYNTHETICALLY ACTIVE RADIATION

The fAPAR (fraction of Absorbed Photosynthetically Active Radiation) quantifies the fraction of the solar radiation absorbed by live leaves for the photosynthesis activity [RD.70]. Then, it refers only to the green and alive elements of the canopy. The fAPAR depends on the canopy structure, vegetation element optical properties, atmospheric conditions, and angular configuration. fAPAR is recognized as an Essential Climate Variable (ECV) by the Global Climate Observing System (GCOS).

Regarding drought monitoring for agriculture and vegetation growth status, the FAPAR can serve as a proper proxy for greenness and vegetation health. The inter-comparison between fAPAR, SPEI, and soil moisture can to some extent show the ability of FAPAR for drought monitoring [RD.71], as the fAPAR standardized anomaly generally agrees well with soil moisture standardized anomaly and SPEI. In particular, the high correlation appears in highly vegetated areas, which suggests the ability of fAPAR to be useful for agricultural drought monitoring.

ENHANCED VEGETATION INDEX

The Enhanced Vegetation Index (EVI) is similar to Normalized Difference Vegetation Index and can be used to quantify vegetation greenness. However, the EVI is designed to enhance the vegetation signal with improved sensitivity in high biomass regions and improved vegetation monitoring through a de-coupling of the canopy background signal and a reduction in atmosphere influences [RD.72]. The EVI is calculated with the following equation:

$$EVI = G \times \frac{(NIR - Red)}{(NIR + C1\ x\ Red - C2\ x\ Blue + L)}$$

Where NIR/red/blue represents the automatically corrected surface reflectance, L refers to the canopy background adjustment which defines non-linear, differential NIR and red radiant transfer through a canopy, and C1, C2 are the coefficients of the aerosol resistance term. The Value of EVI ranges from -1 to 1. The EVI is very useful in analysing crop yield forecasting, crop growth pattern and mapping the crop phenology, detecting land use land cover target features and to identify stress related to drought over different landscapes.

SOIL-ADJUSTED VEGETATION INDEX

The Soil-Adjusted Vegetation Index (SAVI) is used to correct the Normalized Difference Vegetation Index for the influence of soil brightness in areas where vegetative cover is low. The SAVI is calculated as a ratio between the R and NIR values with a soil brightness correction factor (L) defined as 0.5 to accommodate most land cover types. The SAVI is calculated as following:

$$SAVI = \frac{(1 + L)(NIR - Red)}{(NIR + Red + L)}$$

Where L is a canopy background adjustment factor. An L value of 0.5 in reflectance space was found to minimize soil brightness variations and eliminate the need for additional calibration for different soils. The transformation was found to nearly eliminate soil-induced variations in vegetation indices.

EVAPORATIVE STRESS INDEX

The Evaporative Stress Index (ESI) describes temporal anomalies in evapotranspiration, highlighting areas with anomalously high or low rates of water use across the land surface [RD.74]. Here, ET is retrieved via energy balance using remotely sensed land-surface temperature (LST) time-change signals. LST is a fast-response variable, providing proxy information regarding rapidly evolving surface soil moisture and crop stress conditions at relatively high spatial resolution. The ESI also demonstrates capability for capturing early signals of "flash drought," brought on by extended periods of hot, dry, and windy conditions leading to rapid soil moisture depletion.

FRACTION OF VEGETATION COVER

The Fraction of Vegetation Cover (FCover) defines an important structural property of a plant canopy, which corresponds to the complement to unity of the gap fraction at nadir direction, accounting for the amount of vegetation distributed in a horizontal perspective [RD.75]. Because it is independent from the illumination direction, and it is sensitive to the vegetation amount. FCover is related with the partition between soil and vegetation contribution for emissivity and temperature. This property is necessary for describing land surface processes and surface parameterisation schemes used for climate and weather forecasting. Besides, the FCover is relevant for a wide range of Land Biosphere Applications such as agriculture and forestry, environmental management and land use, hydrology, natural hazards monitoring and management, vegetation-soil dynamics monitoring, drought conditions and fire scar extent.

SOIL MOISTURE ANOMALY

The Soil Moisture Anomaly (SMA) indicator that is implemented in the Copernicus Global Drought Observatory (GDO) is used for determining the start and duration of agricultural drought conditions, which arise when soil moisture availability to plants drops to such a level that it adversely affects crop yield, and hence, agricultural production [RD.76]. The SMA indicator in GDO is derived from anomalies of estimated soil moisture (or soil water) content - which are produced as an ensemble of three datasets: the JRC's in-house LISFLOOD hydrological model [RD.77], the MODIS-derived land surface temperature [RD.78] and ESA combined active/passive microwave skin soil moisture [RD.79]. Details on the use of these datasets for drought detection can be find in Cammalleri et al. [RD.80].

NORMALIZED DIFFERENCE MOISTURE INDEX

Normalized Difference Moisture Index (NDMI) is used to determine vegetation water content [RD.81]. It is calculated

as a ratio between the NIR and SWIR values in traditional fashion. NDMI has the capacity to detect water stress at an early stage. Further, using NDMI to monitor irrigation, especially in areas where crops require more water than nature can supply, helps to significantly improve crop growth. All of this makes NDMI an excellent agricultural tool. Although colloquially NDMI is often compared with the NDWI index, the two should be effectively viewed as different indices. While NDMI and Gao's version of NDWI use the NIR-SWIR combination to detect moisture content in leaves, the McFeeters's NDWI uses the GREEN-NIR combination to highlight water bodies and monitor their turbidity.

NDMI is calculated using the near-infrared (NIR) and the short-wave infrared (SWIR) reflectance:

$$\text{NDMI} = \frac{(NIR - SWIR)}{(NIR + SWIR)}$$

The NIR and SWIR bands were selected for the NDMI band equation to mitigate the effects of illumination and atmosphere. The short-wave infrared spectral channel (SWIR) is sensitive to the vegetation water content and the mesophyll structure of leaves. On the other hand, the near-infrared band (NIR) picks up the bright reflectance off the leaf internal structure and leaf dry matter content. When combined, the accuracy of data on the vegetation water content becomes much higher. Additionally, NDMI is a better deforestation indicator than NDVI thanks to a less abrupt decrease in values. The NDMI has values between -1 and 1. Water stress would be signalled by the negative values approaching -1, while the +1 may indicate waterlogging. Therefore, every value in between will correspond to a slightly different agronomic situation.

VEGETATION CONDITION INDEX

The Vegetation Condition Index (VCI) compares the current NDVI to the range of values observed in the same period in previous years [RD.82]. The VCI is expressed in % and gives an idea where the observed value is situated between the extreme values (minimum and maximum) in the previous years. Lower and higher values indicate bad and good vegetation state conditions, respectively. VCI varies from 0 for extremely unfavourable conditions, to 100 for optimal.

$$VCI = 100 \times \frac{(NDVI - NDVI\ min)}{(NDVI\ \max - NDVI\ min)}$$

NDVI max and NDVI min are multiple year maximum NDVI and minimum NDVI for a pixel with reference to a specific climatology.

TEMPERATURE CONDITION INDEX

The Temperature Condition Index (TCI) is used to determine stress on vegetation caused by temperatures and excessive wetness [RD.82]. Conditions are estimated relative to the maximum and minimum temperatures and modified to reflect different vegetation responses to temperature. TCI varies from 0, for extremely unfavourable conditions to 100 for optimal conditions. TCI was developed based on LST observation from TIR remote sensing.

$$TCI = 100 \times \frac{(BT\ \max - BT)}{(BT\ \max - BT\ min)}$$

The weekly thermal brightness temperature is termed as BT. BT is calculated from every week's satellite data of around 17 years i.e., from 2002 to current. BT max and BT min are termed as multiple year maximum and minimum, pixel specific thermal brightness temperature

VEGETATION HEALTH INDEX

The Vegetation Health Index (VHI) illustrates the severity of drought based on the vegetation health and the influence of temperature on plant conditions [RD.83]. The VHI is a composite index and the elementary indicator used to compute seasonal drought indicators. VHI combines both the Vegetation Condition Index VCI and the Temperature Condition Index (TCI). The TCI is calculated using a similar equation to the VCI but relates the current temperature to the long-term maximum and minimum, as it is assumed that higher temperatures tend to cause a deterioration in vegetation conditions. A decrease in the VHI would, for example, indicate relatively poor vegetation conditions and warmer temperatures, signifying stressed vegetation conditions, and over a longer period would be indicative of drought.

STANDARDIZED PRECIPITATION INDEX

The Standardized Precipitation Index (SPI) is the most commonly used indicator worldwide for detecting and characterizing meteorological droughts. The SPI indicator, which was developed by McKee et al. [RD.84], and described in detail by Edwards and McKee [RD.85], measures precipitation anomalies at a given location, based on a comparison of observed total precipitation amounts for an accumulation period of interest (e.g. 1, 3, 12, 48 months), with the long-term historic rainfall record for that period. The historic record is fitted to a probability distribution (the "gamma" distribution), which is then transformed into a normal distribution such that the mean SPI value for that location and period is zero. For any given region, increasingly severe rainfall deficits (i.e., meteorological droughts) are indicated as SPI decreases below –1.0, while increasingly severe excess rainfall are indicated as SPI increases above 1.0. Because SPI values are in units of standard deviation from the long-term mean, the indicator can be used to compare precipitation anomalies for any geographic location and for any number of time-scales. Note that the name of the indicator is usually modified to include the accumulation period. Thus, SPI-3 and SPI-12, for example, refer to accumulation periods of three and twelve months, respectively. The World Meteorological Organization has recommended that the SPI be used by all National Meteorological and Hydrological Services around the world to characterize meteorological droughts [RD.86]. The long-term gamma distribution of our product is based on data from a reference period from 1981 to 2010. The data included in the SPI-48 (4 years SPI) are thus based on monthly rainfall input data from 1978 until 2010.

STANDARDIZED PRECIPITATION EVAPOTRANSPIRATION INDEX

The Standardized Precipitation Evapotranspiration Index (SPEI) is an extension of the widely used Standardized Precipitation Index (SPI) [RD.87]]. The SPEI is designed to take into account both precipitation and potential evapotranspiration (PET) in determining drought. Thus, unlike the SPI, the SPEI captures the main impact of increased temperatures on water demand. Like the SPI, the SPEI can

be calculated on a range of timescales from 1-48 months. At longer timescales (>~18 months), the SPEI has been shown to correlate with the self-calibrating PDSI. If only limited data are available, i.e., temperature and precipitation, PET can be estimated with the simple Thornthwaite method. In this simplified approach, variables that can affect PET such as wind speed, surface humidity and solar radiation are not accounted for. In cases where more data are available, a more sophisticated method to calculate. PET is often preferred to make a more complete accounting of drought variability. However, these additional variables can have large uncertainties.

3.3. INTERNATIONAL AND NON-GOVERNMENTAL EARLY WARNING SYSTEMS

The following chapter presents an overview of operational drought early warning systems (in no particular order).

3.3.1.FAO/WFP WAPOR

Currently in its second phase, WaPOR 2, the project builds on the efforts and accomplishments that were obtained in the first phase, WaPOR 1, which ended in January 2021. Agriculture being a key water user, careful monitoring of water productivity in this sector and exploring opportunities to increase it are imperative measures to counter the increased pressure that it puts on water resources. WaPOR [RD.96], FAO's portal to monitor Water Productivity through Open access of Remotely sensed derived data, assists countries in monitoring water productivity, identifying water productivity gaps, proposing solutions to reduce them, contributing to a sustainable increase of agricultural production. At the same time, it takes into account ecosystems and the equitable use of water resources, which should eventually lead to an overall reduction of water stress.

By providing near real time pixel information, WaPOR opens the door for service-providers to assist farmers in obtaining more reliable yields and improving their livelihoods. At the same time, irrigation authorities have access to information to modernize their irrigation schemes and government agencies are able to use this information to promote and increase the efficient use of their natural resources Figure 3-7.

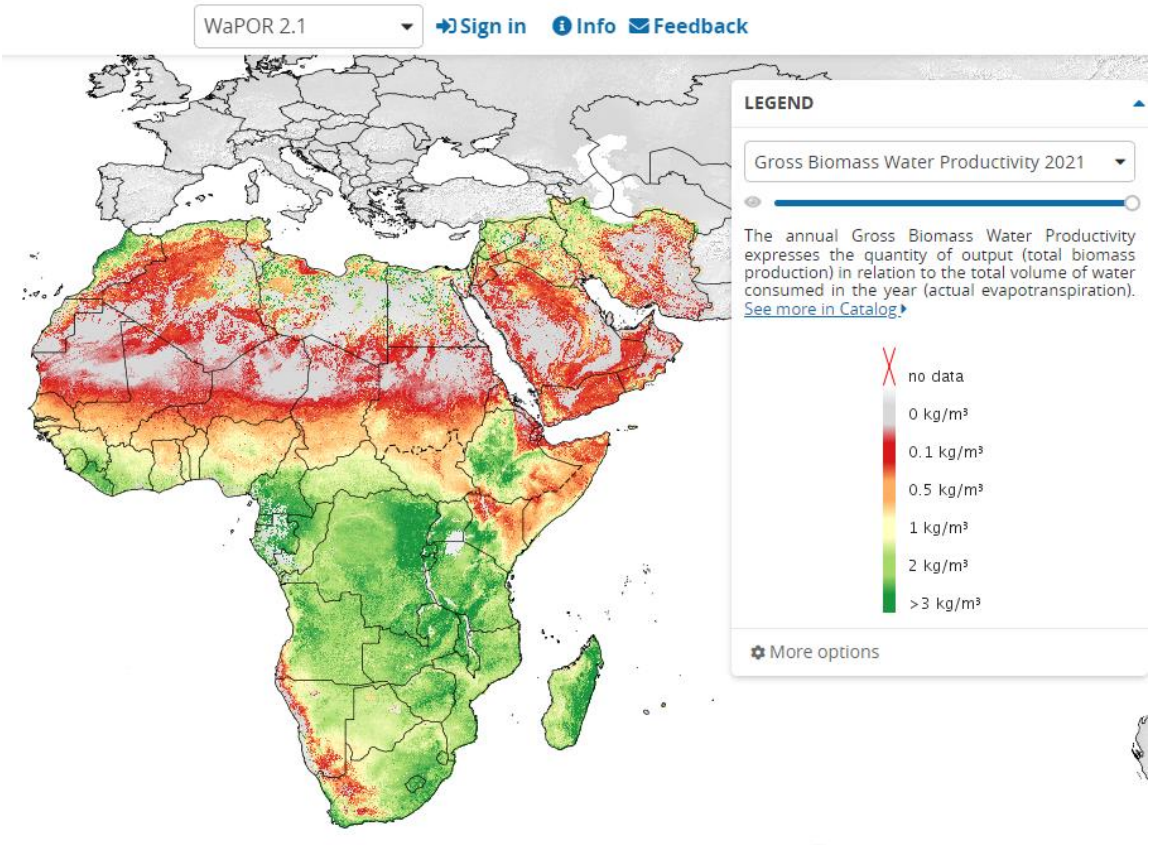

Figure 3-7. WaPOR portal

3.3.2. FEWS NET

FEWS NET, the Famine Early Warning Systems Network, is a leading provider of early warning and analysis on acute food insecurity at global level. Its goal is to strengthen the abilities of countries and regional organizations to manage risk of food insecurity through the provision of timely and analytical early warning and vulnerability information [RD.88]. FEWS NET was created in 1985 by the United States Agency for International Development (USAID) in response to devastating famines in East and West Africa, FEWS NET provides unbiased, evidence-based analysis to governments and relief agencies who plan for and respond to humanitarian crises. FEWS NET analyses support resilience and development programming as well. FEWS NET analysts and specialists work with scientists, government ministries, international agencies, and NGOs to track and publicly report on conditions in the world's most food-insecure countries.

This holistic platform Figure 3-8 utilizes, among a host of other resources, remotely sensed data, and their derived drought/production information, and in situ data to report on food security. These are categorized as early warning indicators and include rainfall estimates, agricultural and climate monitoring products (i.e., SOS, SPI, soil moisture indices, CHIRPS), vegetation index measurements (i.e., NDVI) and climate forecasts. The intended audience of FEWS NET includes global, strategic decision makers, including those at USAID headquarters, decision makers of donor national governments, United Nations agency headquarters, headquarters of key NGOs and national and regional decision makers, such as those of regional offices of USAID, donor NGOs regional offices, UN agencies regional offices, affected national governments, and communities.

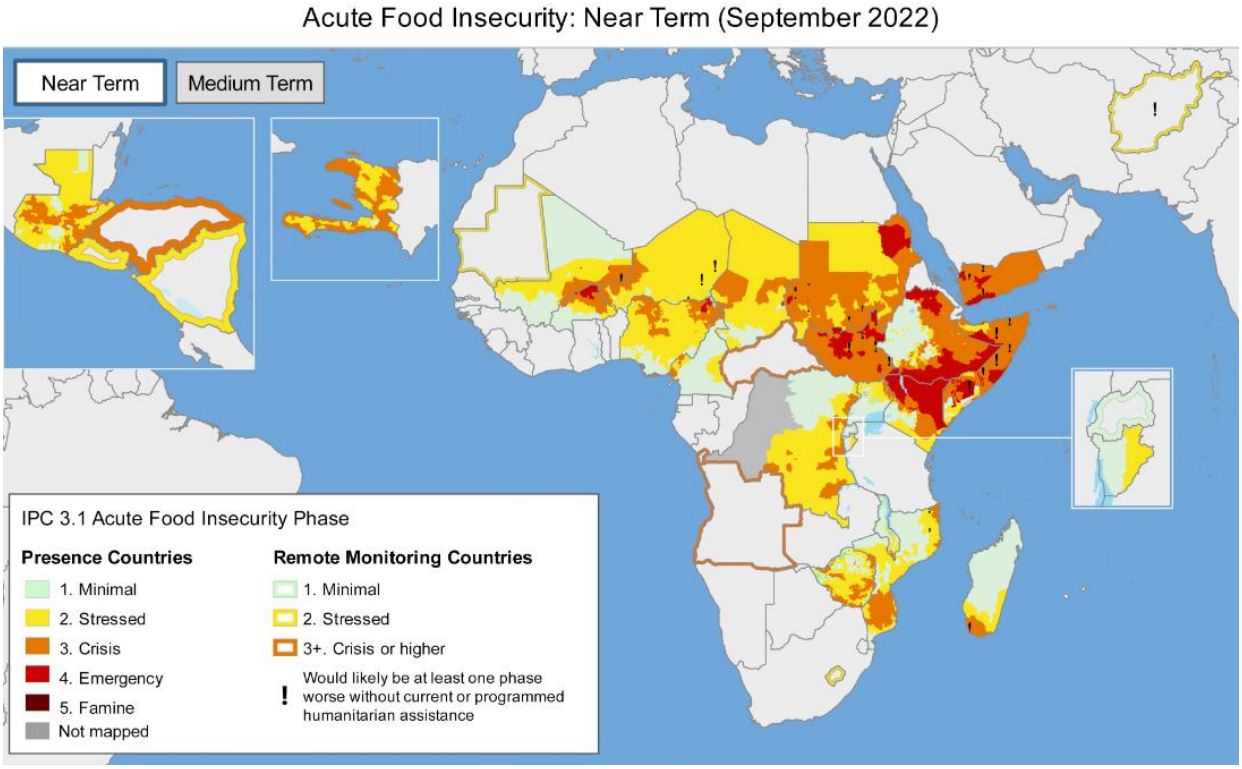

Figure 3-8. FEWS NET portal

3.3.3.US DROUGHT MONITOR

The U.S. Drought Monitor (USDM) published a new map every Thursday, only covering parts of the U.S. that are in drought and labels them by intensity [RD.93], Figure 3-9. The categories are displayed at Figure 3-10. D1 is the least intense level and D4 the most intense. Drought is defined as a moisture

deficit bad enough to have social, environmental, or economic effects. D0 represent areas that are not strictly in drought but are experiencing abnormally dry conditions that could turn into drought or are recovering from drought but are not yet back to normal. The primary physical effects are classified into short- or long-term droughts:

- S = Short-term, typically less than 6 months (agriculture, grasslands)
- L = Long-term, typically more than 6 months (hydrology, ecology)
- SL = Area contains both short- and long-term impacts

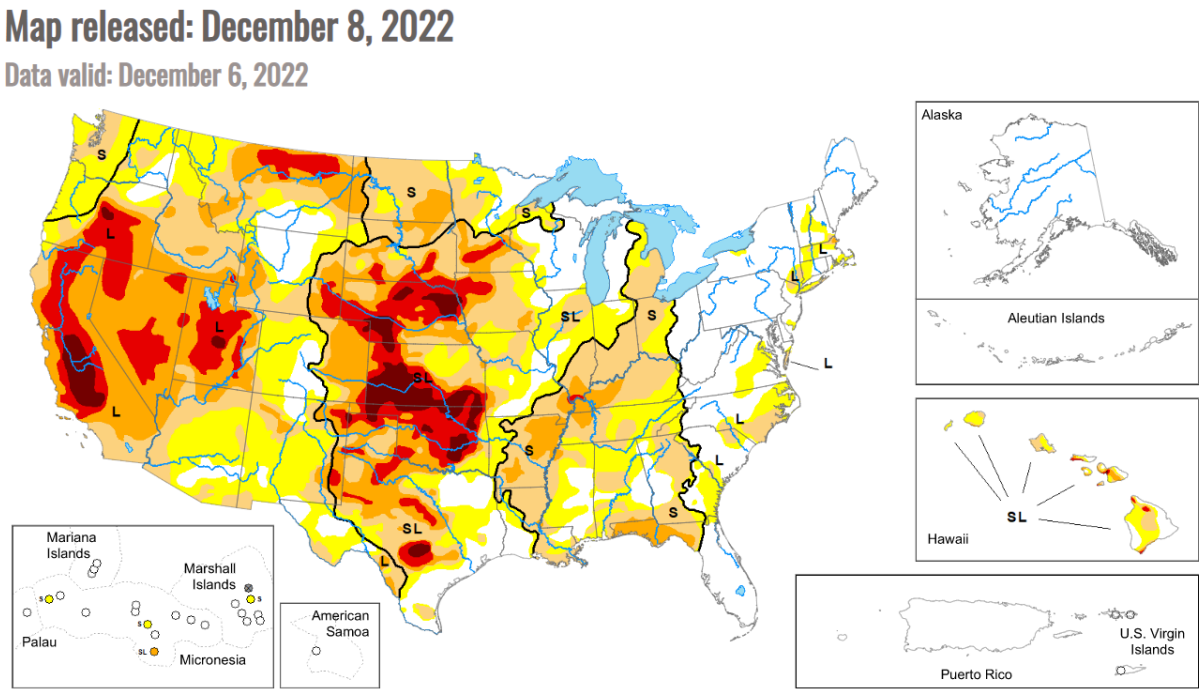

Figure 3-9. US Drought Monitor.

While drought intensity categories are based on the original five key indicators along with several dozen other objective indicators local condition reports and impact reports from more than 450 expert observers around the country drought impacts which subjectively support and validate the indicators used.

Category	Description	Possible Impacts	Ranges				
			Palmer Drought Severity Index (PDSI)	CPC Soil Moisture Model (Percentiles)	USGS Weekly Streamflow (Percentiles)	Standardized Precipitation Index (SPI)	Objective Drought Indicator Blends (Percentiles)
D0	Abnormally Dry	Going into drought: • short-term dryness slowing planting, growth of crops or pastures Coming out of drought: • some lingering water deficits • pastures or crops not fully recovered	-1.0 to -1.9	21 to 30	21 to 30	-0.5 to -0.7	21 to 30
D1	Moderate Drought	• Some damage to crops, pastures • Streams, reservoirs, or wells low, some water shortages developing or imminent • Voluntary water-use restrictions requested	-2.0 to -2.9	11 to 20	11 to 20	-0.8 to -1.2	11 to 20
D2	Severe Drought	• Crop or pasture losses likely • Water shortages common • Water restrictions imposed	-3.0 to -3.9	6 to 10	6 to 10	-1.3 to -1.5	6 to 10
D3	Extreme Drought	• Major crop/pasture losses • Widespread water shortages or restrictions	-4.0 to -4.9	3 to 5	3 to 5	-1.6 to -1.9	3 to 5
D4	Exceptional Drought	• Exceptional and widespread crop/pasture losses • Shortages of water in reservoirs, streams, and wells creating water emergencies	-5.0 or less	0 to 2	0 to 2	-2.0 or less	0 to 2

Figure 3-10. Drought classification

The drought severity classification table shows the ranges for each indicator for each dryness level. Because the ranges of the various indicators often don't coincide, the final drought category tends to be based on what most of the indicators show and on local observations. The analysts producing the map also weigh the indices according to how well they perform in various parts of the country and at different times of the year. It is this combination of the best available data, local observations and experts' best judgement that makes the U.S. Drought Monitor more versatile than other drought indicators.

Short-term drought indicator blends focus on 1–3-month precipitation. Long-term blends focus on 6-60 months. Additional indices used, mainly during the growing season, include the USDA/NASS Topsoil Moisture, Keetch-Byram Drought Index (KBDI), and NOAA/NESDIS satellite Vegetation Health Indices. Indices used primarily during the snow season and in the West include snow water content, river basin precipitation, and the Surface Water Supply Index (SWSI). Other indicators include groundwater levels, reservoir storage, and pasture/range conditions.

The U.S. Drought Monitor provides a consistent big picture look at drought conditions in the United States. Although it is based on many types of data, including observations from local experts across the country, it is not intended to obtain specifics about local conditions. It can certainly be used to identify likely areas of drought impacts, including water shortage, but decision-makers in many circumstances have successfully taken measures to reduce vulnerability to drought. Large urban water systems generally have diverse water supplies and can keep the water flowing in both dry and wet years.

3.3.4. EUROPEAN DROUGHT OBSERVATORY

The European Drought Observatory (EDO) platform contains drought-relevant information such as maps of indicators derived from different data sources (e.g., precipitation measurements, satellite measurements, modelled soil moisture content). Different tools allow for displaying and analysing the information and drought reports give an overview of the situation in case of imminent droughts Figure 3-11.

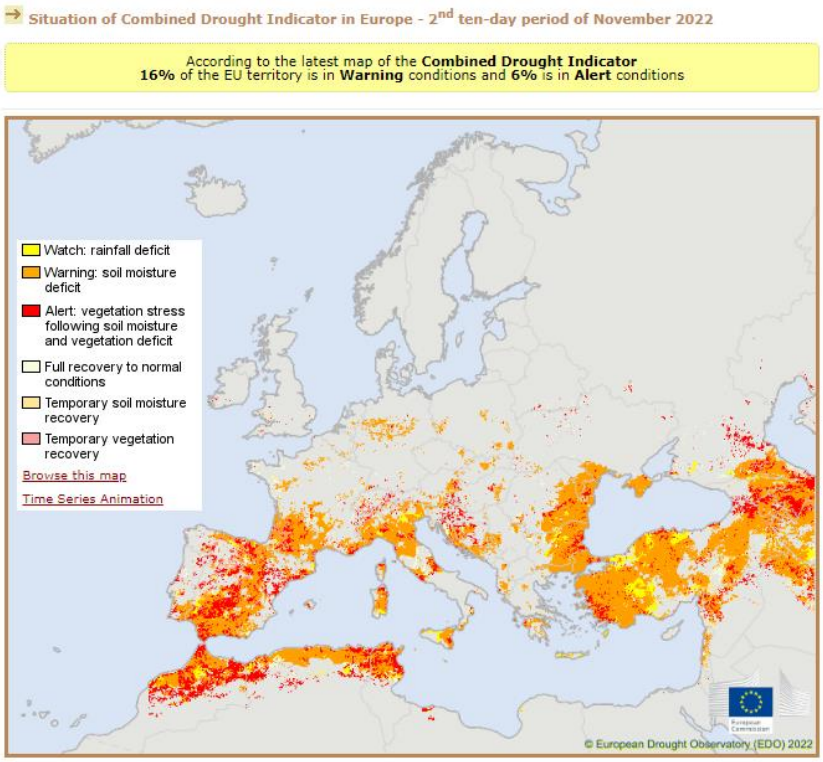

Figure 3-11. European Drought Observatory

At a European scale, the Combined Drought Indicator (CDI) provides a concise representation of the evolution of agricultural droughts, suitable for communication to both specialized end users, policymakers, and the general public [RD.90]. The CDI has been successfully applied within the European Drought Observatory of the EU's Copernicus Emergency Management Service, as part of a near-real-time monitoring with dekadal (roughly 10d, 3 times per month) updates and a time lag of just a few days. The CDI is derived by combining three drought indicators: the Standardized Precipitation Index (SPI), the Soil Moisture Anomaly (SMA), and the FAPAR Anomaly. The CDI classifies areas according to three primary drought classes: "Watch", indicating that precipitation is less than normal; "Warning", indicating that soil moisture is in deficit; and "Alert", indicating that vegetation shows signs of stress. Two additional classes-namely "Partial recovery" and "Recovery" -identify the stages of the vegetation recovery process. Platforms such as the Global Drought Observatory (GDO) [RD.91] and the East Africa Drought Watch [RD.91] were developed by the team of the European Drought Observatory and apply similar methods.

3.4. SOUTH AFRICAN DROUGHT INFORMATION SYSTEMS

3.4.1. NIWIS

The National Integrated Water Information System (NIWIS) was developed by the Department of Water and Sanitation of South Africa with the purpose of providing information products, in the form of dashboards, to facilitate efficient analysis and reporting across the water value chain in South Africa [RD.94]. The Drought Status and Management information system is designed to provide regular overview and outlook of drought status in South Africa. The Drought Status and Management dashboard currently integrates rainfall, river flow, dam level and groundwater level data as the main indicators for generating drought status information Figure 3-12. Other indicators such as vegetation condition are intended to be added in the future.

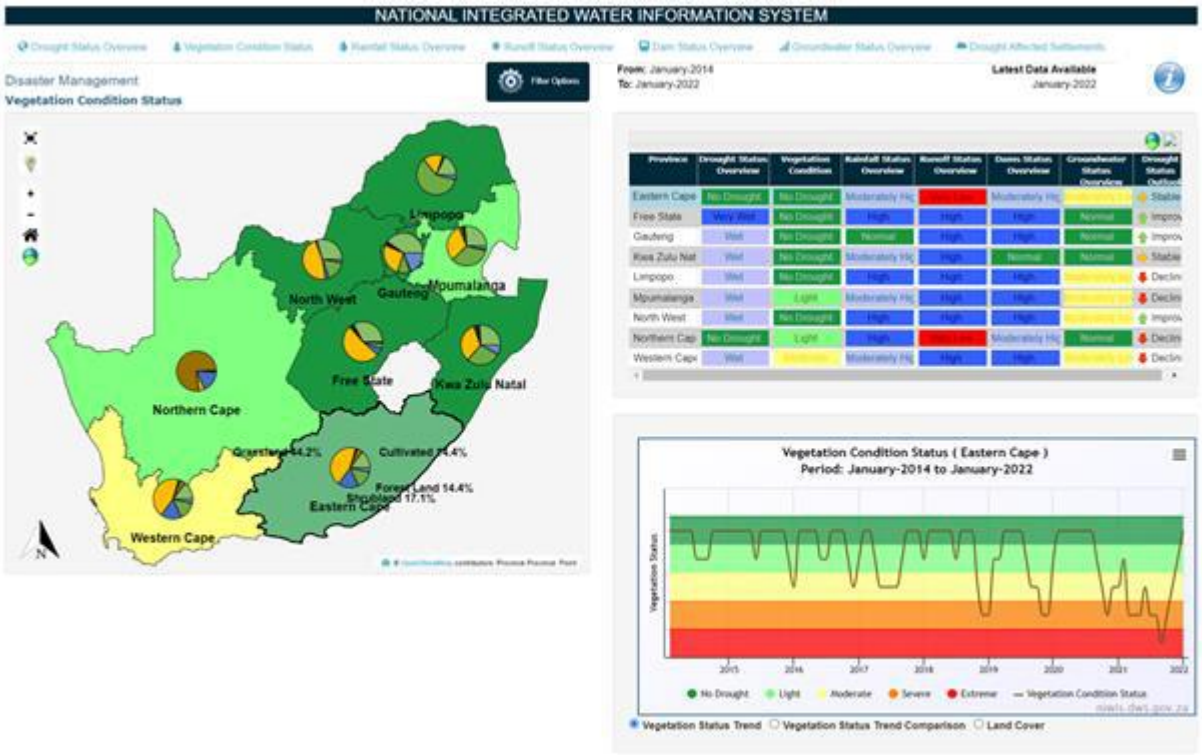

Figure 3-12. NIWIS portal

Drought Status Overview relates to the assessments of impact of drought and risks management. In order to monitor and manage drought risk, the specific indicators such as precipitation, streamflow, reservoir levels, groundwater levels, and vegetation condition may be used. Providing integrated information derived from various indicators. The Drought Status information system is designed to provide regular overview and outlook of drought status in South Africa to water sector decision makers, as well sector wide stakeholders.

In the Drought Status dashboard, the Multi Criteria Decision Analysis (MCDA) method is used to integrate rainfall, river flow, dam levels and groundwater level data as the main indicators for generating up to date hydrological drought status information. In addition, the satellite-based vegetation condition index is used to generate up to date agricultural drought status information. The Vegetation Condition Index (VCI) is based on the comparative Normalized Difference Vegetation Index change with respect to minimum historical NDVI value. Therefore, the VCI compares the recent Vegetation Index (VI) such as NDVI or Enhanced Vegetation Index (EVI) to the values observed on the same period as in previous years within a specific pixel. The resulting percentage of the observed value is situated between the extreme values (minimum and maximum) in the previous years. Lower and higher values therefore indicate bad and good vegetation state conditions, respectively. The Land cover overview is based on the South African National Land-Cover 2018 dataset (provided by the Department of Environmental Affairs), which was generated from multi-seasonal Sentinel-2 satellite imagery and available under an open-source license agreement.

3.4.2. UMLINDI NEWSLETTER

The Umlindi newsletter, developed by the Agricultural Research Council (ARC), provides information on drought conditions based on the interpretation of satellite and climate data [RD.95]. This information is translated and packaged into monthly newsletters with understandable key messages and disseminated to government, private organizations and the public via the internet and e-mail subscriptions. The information is presented at the monthly Crop Estimates Committee meetings as well as to the National Agrometeorological Committee every three months. Data is also available on request, either in the form of maps or through an open geographical information system (GIS) format.

Umlindi's Earth Observation data and derived products are sourced by the Coarse Resolution Satellite Imagery Database (CRID) facility at ARC- ISCW. The CRID comprises the following satellite imagery databases:

- NOAA AVHRR: ARC-ISCW has an archive of daily NOAA AVHRR data dating from 1985 to 2004. This database includes all 5 bands as well as the Normalized Difference Vegetation Index (NDVI), Active Fire and Land Surface Temperature (LST) images. The NOAA data are used, for example, for crop production and grazing capacity estimation.
- MODIS data is distributed by the Land Processes Distributed Active Archive Center (LP DAAC), located at the US Geological Survey's EROS Data Center. The MODIS sensor is more advanced than NOAA with regard to its high spatial (250 m2 to 1 km2) and spectral resolution. ARC-ISCW has an archive of MODIS v4 from 2000 to 2006 and MODIS v5 from 2000 to present. Datasets include:
    - MOD09 (Surface Reflectance)
    - MOD11 (Land Surface Temperature)
    - MOD13 (Vegetation Products)
    - MOD14 (Active Fire)
    - MOD15 (Leaf Area Index & Fraction of Photosynthetically Active Radiation)
    - MOD17 (Gross Primary Productivity)
    - MCD43 (Albedo & Nadir Reflectance)
    - MCD45 (Burn Scar)
- VGT4AFRICA and GEOSUCCESS. SPOT NDVI data is provided courtesy of the VEGETATION Programme and the VGT4AFRICA project. The European Commission jointly developed the VEGETATION Programme. The VGT4AFRICA project disseminates VEGETATION products in Africa through GEONETCast. ARC-ISCW has an archive of VEGETATION data dating from 1998 to 2008. Other products distributed through VGT4AFRICA and GEOSUCCESS include Net Primary Productivity, Normalized Difference Wetness Index and Dry Matter Productivity data.
- Meteosat Second Generation (MSG). ARC-ISCW has an operational MSG receiving station. Data from April 2005 to the present have been archived. MSG produces data with a 15-minute temporal resolution for the entire African continent. Over South Africa the spatial resolution of the data is in the order of 3 km. The Institute investigated the potential for the development of products for application in agriculture. NDVI, LST and cloud cover products were some of the initial ones derived from the MSG SEVIRI data. Other products derived from MSG used weather station data, including air temperature, humidity and solar radiation.

The following indices derived from the above mentioned EO data sources are part of the Umlindi newsletter.

- 16-day composite MODIS NDVI
- 16-day MODIS NDVI difference map
- Percentage of Average Seasonal Greenness (PASG)
- Vegetation Condition Index (16-day composite) and its deviation from 19 years series mean value

In addition to EO products the following inputs are used to compose the value-added products, alone or in combination with EO data:

- Rainfall maps combine inputs from 450 automatic weather stations from ARC-ISCW, 270 automatic stations form SAWS, satellite rainfall estimates from the Famine Early Warning System Network and long-term average surfaces developed at the ARC-ISCW
- Solar Radiation and Evapotranspiration maps are produced from:
    - Combines 450 automatic weather stations from ARC-ISCW network
    - Data from the METEOSAT Second Generation (MSG) 3 satellite via GEONETCast

3.5. GAP ANALYSIS

The following objectives are stated in the National Integrated Water Information System - DWS - NIWIS - Disaster Management, for an overview see chapter 3.4.1

- delivering data products in the form of dashboards to facilitate efficient analysis, and
- reporting throughout the South African water value chain

This brief section aims to assess whether the objectives have been met and which potential enhancements should be considered. The NIWIS Drought Status and Management information system integrates main indicators:

- rainfall,
- river flow,
- dam level and
- groundwater level data

Other indicators such as vegetation condition are planned to be added in the future.

3.5.1. Drought Status Overview

When analysing the NIWIS drought status dashboard Figure 3-13 we determined that:

- Resolution: the data is provided at low resolution
- Scale: each province is evaluated as a unit.

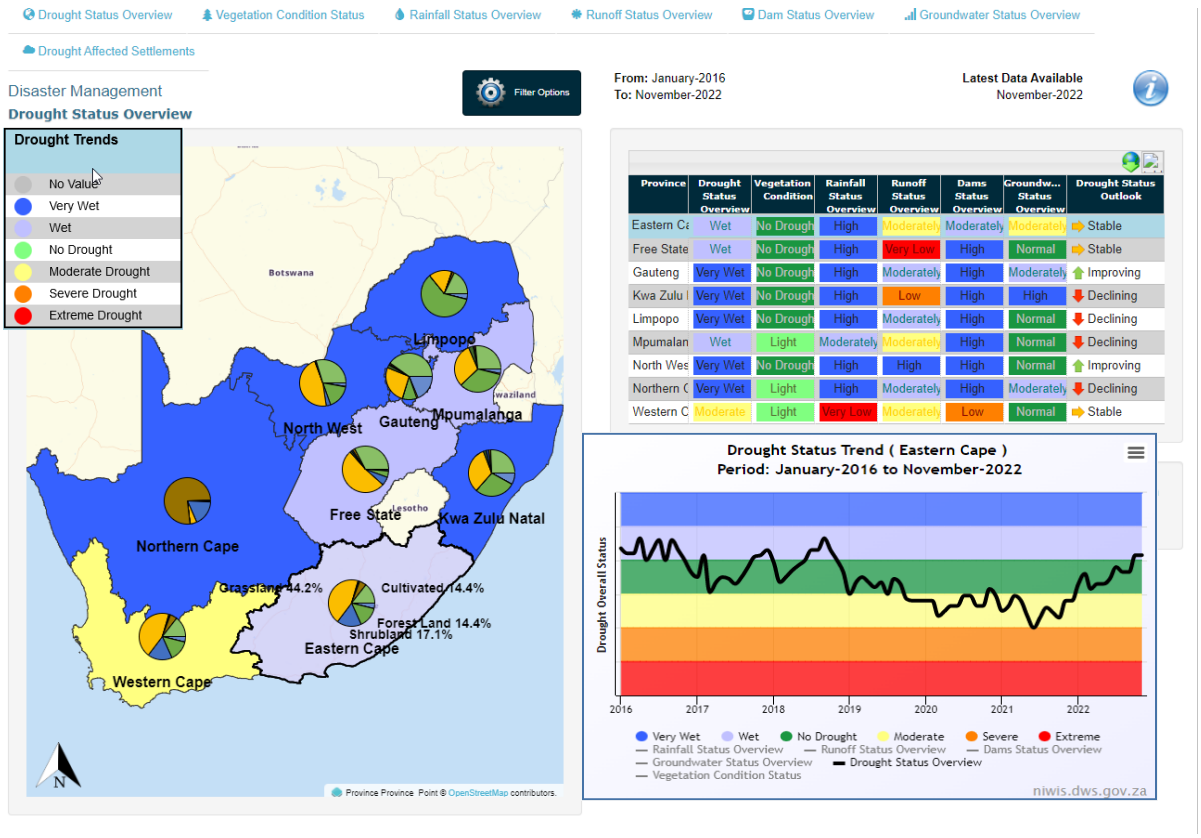

Figure 3-13. NIWIS drought status overview

CONCLUSION: the status of drought at the provincial level does not provide the quantity and quality of information necessary to make accurate decisions, such as where and how many resources should be allocated for effective aid. The spatial resolution should be increased.

3.5.2. Rainfall Status

We made de following observations for the rainfall status overview dashboard [Figure 3-14]:

- Timeliness: the last update of the rainfall status is from July 2022.
- Forecasting: a forecast system cannot be found.
- Scale: evaluation is made at provincial scale.

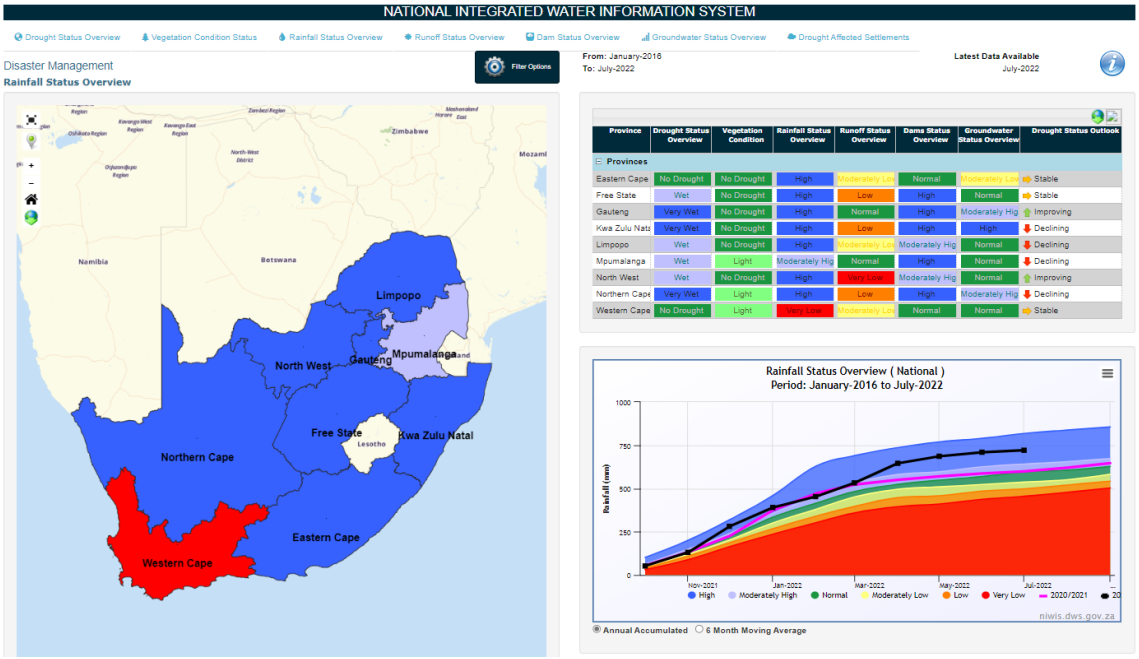

Figure 3-14. NIWIS rainfall status

As in the previous instance, the rainfall status is evaluated on a provincial scale, and as we saw in the prior case, a single province can have distinct environmental characteristics (combination of soil, topography, precipitation, etc.). In this case, a province on the eastern side of the country can observe a wide range of annual precipitation. In this sense, the evaluation should be done at the same scale of the annual precipitation. See the image illustrating the annual precipitation distribution in South Africa [Figure 3-15]. However, to make timely decisions, we must be aware of the most likely precipitation scenarios for at least the current season and the next. In other words, within the subsequent 30 days and three months (synoptic time scales).

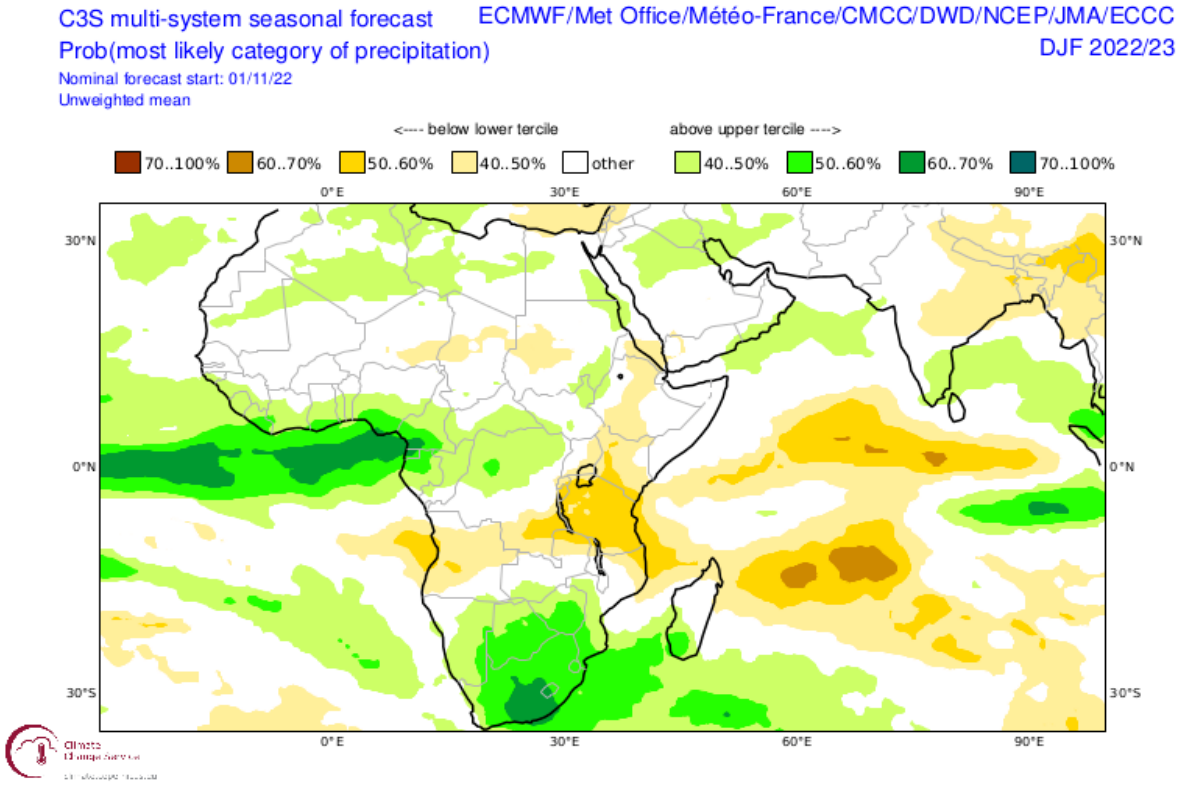

Figure 3-15 C3S seasonal precipitation.

CONCLUSION: The actual system lacks this forecast component. Nowadays, several models and systems exist (see section 0). For instance, the COPERNICUS system uses 9 different models. From these, for instance, the most suitable one for South Africa should be evaluated [Figure 3-16].

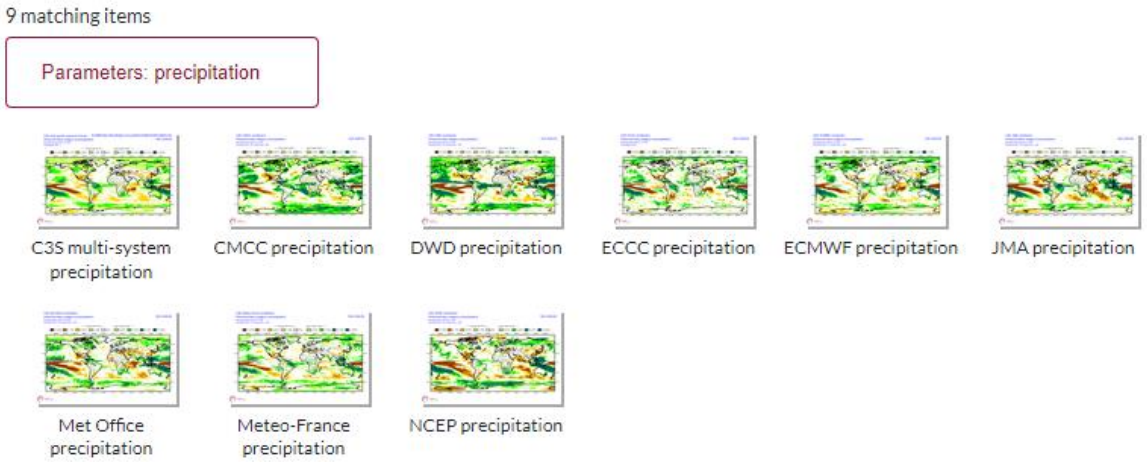

Figure 3-16. Copernicus precipitation models

3.5.3. Groundwater Status

We made de following observations for the groundwater status dashboard Figure 3-17:

- Timeliness: the last update of the rainfall status is from May 2022.

- Scale: evaluation is made at provincial scale.

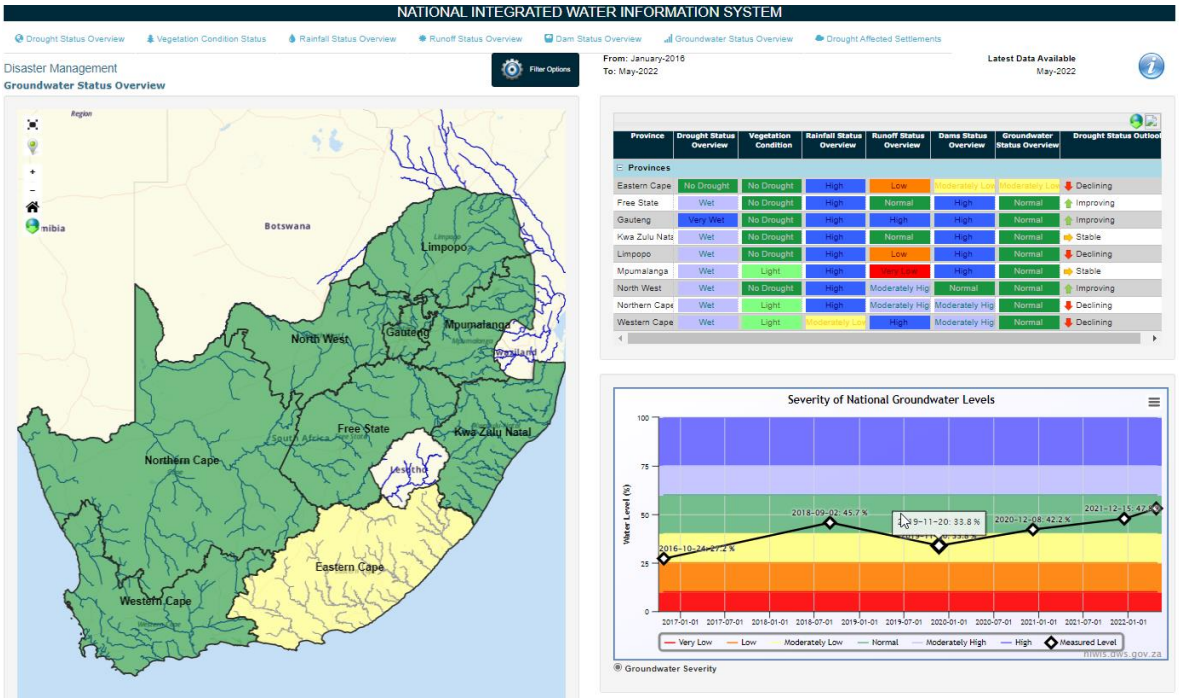

Figure 3-17. NIWIS groundwater status.

Groundwater systems are intricate systems based on geological and tectonic factors spanning eons. The image below, derived from satellite data as part of the ESA's Earth Observation for Sustainable Development project, demonstrates that drought risk is not uniformly distributed across large areas and can vary over short distances.

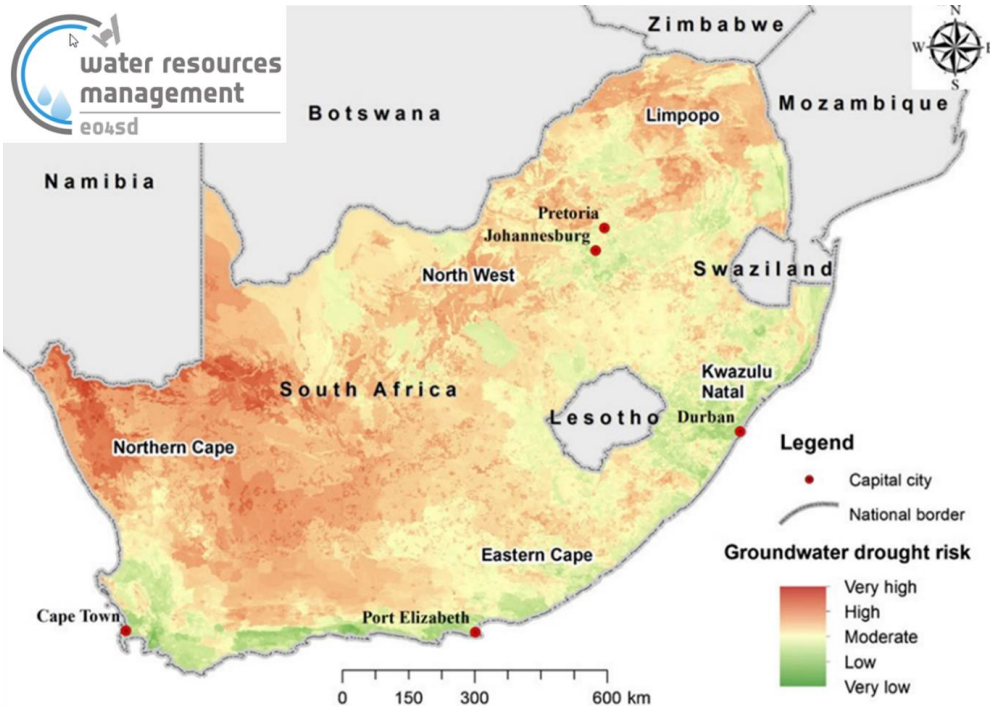

Figure 3-18. EO4SD Groundwater drought risk.

CONCLUSION: Since groundwater systems are below the surface, it is very expensive to obtain in situ data on a single point. This gets worse if the variability of the system is high as shown above. Therefore, remote sensing nowadays provides valuable data that should be used and incorporated into DWS system. The image below, derived from the twin-satellites GRACE FO, shows how the water volume, in terms of percentile, has varied since January 2017 to December 2022 Figure 3-19.

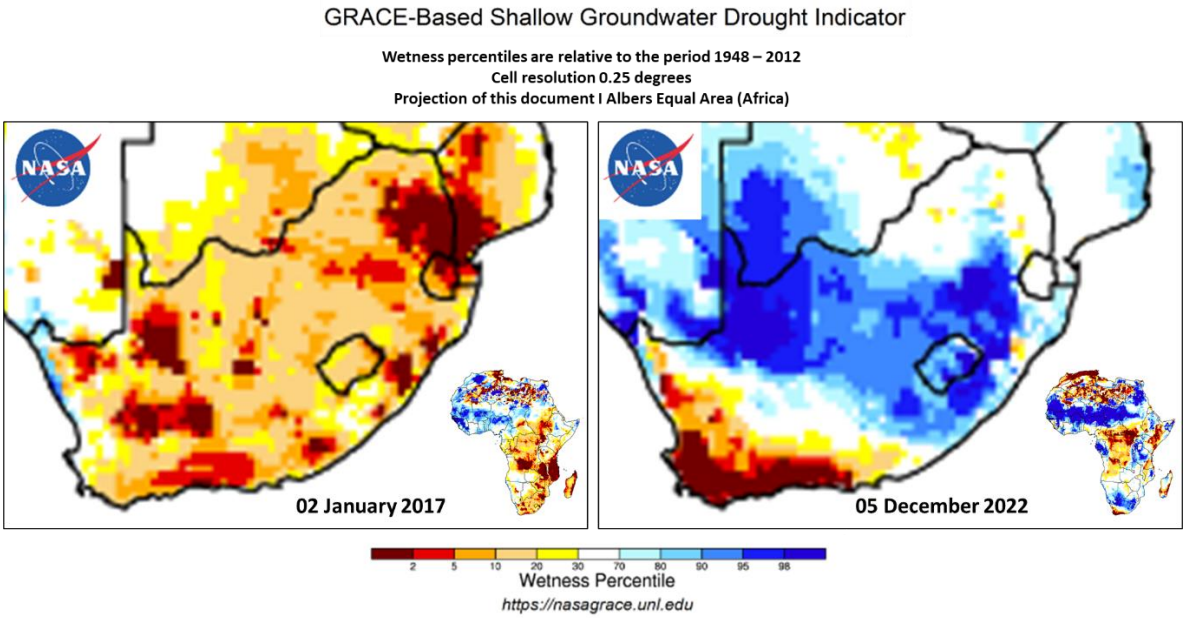

Figure 3-19. NASA GRACE shallow ground water drought indicator.

Root Zone Soil Moisture: The first meter of the soil's surface is commonly referred to as the root zone because it contains the plant's radicular systems. This soil layer's water content sustains most of the crop. Monitoring this variable, in close to real-time, is a crucial factor in determining drought conditions. While changes in groundwater systems are slow and can take several days, weeks, or even months, depending on the depth of the water table, changes in the root zone can occur within hours or days, emphasizing the importance of monitoring this variable closely. The graph below depicts the evolution of these variables.

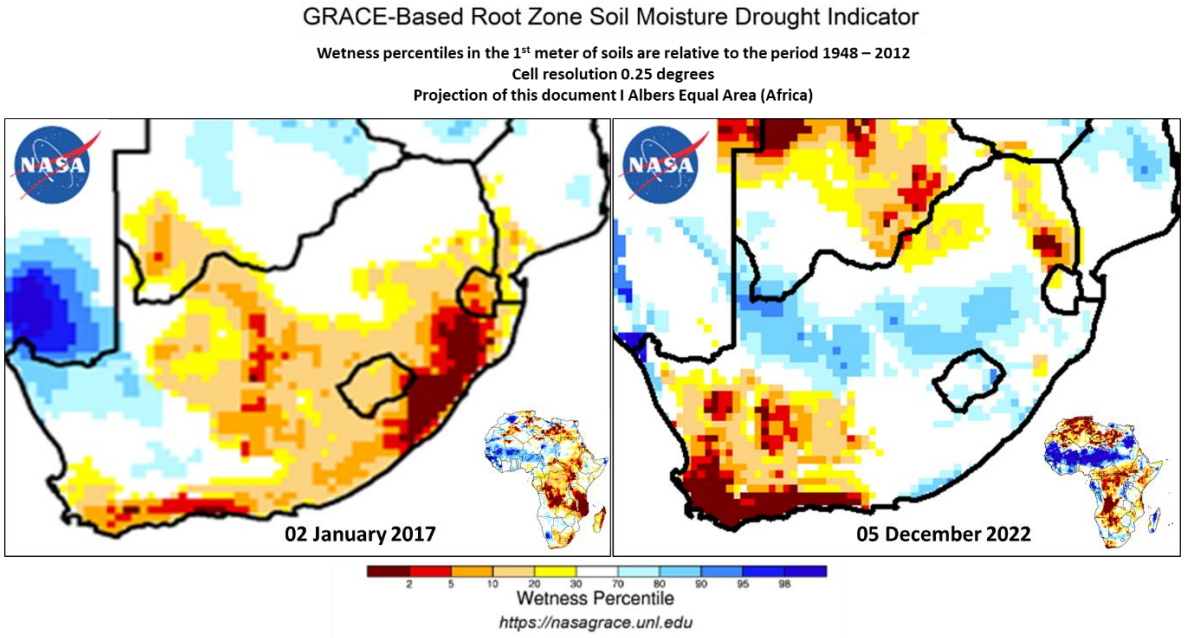

Figure 3-20. NASA GRACE root zone soil moisture drought indicator.

3.6. CONCLUSIONS

Although, the current implementation of NIWIS has broken ground and already provides vital information to local stakeholders. We conclude that the NIWIS drought monitoring system can be significantly improved and propose the following:

- Increase the scale and report on municipal or watershed level, as generalized provincial results (9 provinces see Figure 3-14) are not capable of reflecting on the variability at local level (257 municipalities).
- Integrate data on soils, agroecological zones or annual precipitation trends to further improve the results as they can have a substantial impact on drought and water requirements.
- Revise the current models to retrieve drought information and updated these with state-of-the-art data such as up to date precipitation, ground water, soil moisture and temperature data. This would also enable the system to make predictions on drought.
- Update the UI to provide a better user experience.

By performing these proposed improvements, the NIWIS 2.0 system would gain additional functionalities which can be found in drought monitoring platforms such as WAPOR, FEWS NET or the US Drought Monitor. These results will be presented to the South African partners for review and a jointly developed user driven solution will be implemented in the later stages of the project.

END OF DOCUMENT

